NACA RM L50B03

NACA

RESEARCH MEMORANDUM

FLIGHT INVESTIGATION OF THE PRESSURE DISTRIBUTIONS AND LOADS ON A FRONT AND REAR SLIDING CANOPY

By Wilber B. Huston and T. H. Skopinski

Langley Aeronautical Laboratory
Langley Air Force Base, Va.

NATIONAL ADVISORY COMMITTEE
FOR AERONAUTICS

WASHINGTON
April 4, 1950

NACA RM L50B03

NATIONAL ADVISORY COMMITTEE FOR AERONAUTICS

RESEARCH MEMORANDUM

FLIGHT INVESTIGATION OF THE PRESSURE DISTRIBUTIONS AND LOADS ON A FRONT AND REAR SLIDING CANOPY

By Wilber B. Huston and T. H. Skopinski

SUMMARY

Pressure-distribution measurements and load-coefficient data at low speeds obtained in flight for a conventional front and rear sliding canopy are presented. The data were obtained with the same canopy previously tested in the Langley full-scale tunnel. The flight measurements show good agreement with the full-scale-tunnel results for comparable conditions and confirm the principal conclusions of the tunnel tests as to the effect of canopy position, yaw, power, and lift coefficient on the pressure distributions. Any changes in load distribution which might be due to distortion of the canopies under load were within the limits of the experimental error. The load-coefficient data indicate that the highest net aerodynamic load for the front canopy was in the exploding direction and occurred with the front and rear canopies closed. The highest net load for the rear canopy was in the crushing direction with the front canopy open and rear canopy closed.

INTRODUCTION

An investigation of the aerodynamic loads on airplane canopies and cockpit enclosures has been conducted at the Langley Laboratory. The first phase of this investigation included low-speed tests in the Langley full-scale tunnel on three conventional enclosures representative of the three categories, single sliding canopy, front and rear sliding canopy, and bubble-type canopy. Pressures over the external and internal surfaces of the canopies were measured under a wide range of operating conditions, and the data have been reported in references 1 to 3.

The second phase of the investigation included flight tests of two of the canopies tested to obtain a qualitative comparison of flight and wind-tunnel results, and to determine the severity of the effects of

Mach number and of distortion. Loads on the bubble-type canopy at low speeds and data on the effect of Mach number have been reported in reference 4. Data on internal cockpit pressures are reported in reference 5. In the present paper, pressure distributions and load coefficients for the front and rear sliding canopies of the SB2C-4E airplane obtained at low speeds and data on the effect of distortion are given. Data were obtained under steady-state conditions at lift coefficients ranging from 0.17 to 1.33, at yaw angles of 0°, -7.5°, and 7.5°, and at pressure altitudes of 8,000 and 20,000 feet. The Mach number ranged from 0.146 to 0.44.

SYMBOLS

A	cross-sectional area of canopy normal to plane of symmetry (see fig. 5)
C_y	canopy lateral load coefficient (L_y/qA)
C_z	canopy vertical load coefficient (L_z/qA)
C_L	airplane lift coefficient
D	propeller diameter, feet
h_p	pressure altitude, feet
L	canopy load, pounds
M	Mach number
p	pressure, pounds per square foot
P	pressure coefficient $\left(\frac{p - p_o}{q}\right)$
q	free-stream dynamic pressure, pounds per square foot ($0.7p_oM^2$)
Q	torque, pound-feet
Q_c	torque coefficient $\left(\frac{Q}{2qD^3}\right)$
T	thrust, pounds

T_c thrust coefficient $\left(\frac{T}{2qD^2}\right)$

Δ increment due to yaw

ψ yaw angle, degrees

Subscripts:

e external

i internal

o free stream

L left side of canopy

R right side of canopy

y lateral

z vertical

f front

r rear

APPARATUS

Airplane.— The airplane (fig. 1) used in the tests was a single-engine, two-place, low-wing scout and dive bomber for use aboard aircraft carriers. The gross weight of the airplane during the flight tests was about 13,000 pounds; the wing area was about 422 square feet, corresponding to a wing loading of 30.8 pounds per square foot. With the exception of the addition of booms on the right and left wing tips for airspeed and yaw instrumentation, there were no external modifications to the airplane. The airplane was powered by an R-2600-20 Wright engine with a military rating at 2600 rpm of 1720 and 1560 brake horsepower at sea level and 8000 feet, respectively, while at 20,000 feet, 1180 brake horsepower was developed at 2300 rpm. The engine-propeller gear ratio was 16:9. The propeller had four blades and a diameter of 12 feet 2 inches and was a Curtiss electric constant-speed propeller with blades of design No. C2721200(American). At military power the propeller operated at the conditions of thrust and torque shown in figure 2.

The front and rear sliding canopies (fig. 3) are each mounted on four carriers that roll on tracks designed to raise the canopies slightly and at the same time direct them over the stationary canopy. When fully opened, the front and rear canopies are raised $2\frac{1}{4}$ and $1\frac{1}{4}$ inches, respectively, above the top of the stationary canopy. The front canopy slides to the rear while the rear canopy slides forward as shown by figure 3. The front canopy is made up of two plexiglass panels 1/4 inch thick and is equipped with a quick-release jettisoning latch. The rear canopy consists of a number of plexiglass panels 1/8 inch thick and, in addition to a built-in emergency hatch, is equipped with a hinged deflector on each side (fig. 4), which extends outward about 50° when the canopy is in the full-open position. With the rear canopy closed, the deflectors retract flush with the sides except for the small tip or radius on the trailing edge evident in figure 4(b). The sliding canopies were the same ones used in the full-scale-tunnel investigation (reference 2). A line drawing of the canopies (fig. 5) shows the contours and principal dimensions.

Instrumentation.- Standard NACA instrumentation was used to measure airspeed, pressure altitude, normal acceleration, angle of yaw, local static pressures, and time. The pitot-static tube and yaw head were mounted on booms located approximately 1 chord ahead of the wing leading edge. The yaw-angle recorder was also connected to an indicator in the cockpit for the pilot's use.

For the survey of local static pressure over the exterior of the front and rear canopies, the stationary canopy, and the turtle deck, 115 flush orifices were installed at the locations shown in figure 5. For internal pressures, an orifice was located in both the front and rear cockpits. The orifices at stations 7, 9, 10, and 11, which are directly under the front and rear canopies in the open position, were also used.

Pressures at 112 of the 117 survey locations were measured by seven standard NACA two-capsule pressure recorders, utilizing a motor-driven selector switch. Data were taken during stabilized runs of 30 seconds duration, each orifice being sampled for a 3-second interval. A continuous record was obtained of the front and rear cockpit pressures and, as a check on the selector, of three external orifices. All pressures were obtained relative to free-stream static pressure as given by the pitot-static tube, and a correction was made for the difference between true and measured free-stream static pressure based on a flight calibration of the airspeed system. Pressure tubing of $\frac{3}{16}$-inch inside diameter was used for all connections. The pressure lines between the orifices and the instruments located in the bomb bay were 15 to 20 feet in length.

Accuracy.— The precision of directly measured and derived quantities given in the present paper is believed to lie within the following precision estimates:

$p - p_o$	±0.2 inch of water
C_L	±2 percent
M	±0.007
T_c	±5 percent
P	±2 percent
ψ	±0.5
C_z, C_y	less than ±5 percent

The precision given for P is based on the average uncertainties in determining both $p - p_o$ and q. The precision given for C_z and C_y is based on estimates of possible errors introduced by fairing data, by the integrating process, and by the uncertainty in P.

TEST PROCEDURE AND METHODS

Flight Program

The flight program for obtaining data on canopy loads was planned to duplicate certain of the flight and operating conditions for which tests were reported in reference 2. Flights were therefore made at different airspeeds corresponding to lift-coefficient values of 0.17, 0.56, 0.98, and 1.33, representing a high speed, a take-off, and two intermediate flight conditions. Since it was not always possible to obtain the four nominal values of C_L exactly, actual values of lift coefficient have been used where data are plotted as a function of C_L. Tests were made at military power at these four C_L values, and with the propeller idling at a C_L of 1.33. Flights were made at a uniform pressure altitude of 8000 feet, and since the instrumentation required stabilized conditions during any one run, all tests were made in steady sideslips, in steady level flight, or in steady shallow dives at about 1 g. All tests, except those at $C_L = 0.17$ were made at yaw angles of 0°, −7.5° (yaw to left, right wing advanced), and 7.5° (yaw to right, left wing advanced). Canopy positions investigated at the three higher values of C_L were as follows: With the rear canopy open, the front canopy was closed, 3 inches open, one-half open, and full open; with the rear canopy closed, the front canopy was closed and full open. At $C_L = 0.17$, tests were made with the rear canopy open, the front canopy closed, 3 inches open, and full open.

In order to determine whether under changes in load there were changes in load distribution which could be ascribed to distortion of the canopy, three additional runs were made at a reduced value of dynamic pressure, but otherwise at flow conditions which were as nearly equivalent as it is possible to obtain in flight at 1 g. These runs were made at 20,000 feet at the Mach number of the high-speed, low-lift-coefficient condition at 8,000 feet. Data were thus obtained at dynamic pressures of 213 and 132 pounds per square foot, as compared to the limit value of 415 pounds per square foot corresponding to the maximum permissible diving speed at sea level.

The cockpit ventilator was opened for all runs and the cowl flap positions varied with power. A check of the effect of cowl flap position on the pressure distribution at $C_L = 0.98$ showed that any difference in canopy load due to cowl flap position was within the experimental error.

Evaluation of Canopy Loads

The canopy loads in the present paper are shown in two forms: plots of pressure coefficient P to show the longitudinal and lateral distribution of load; and as load coefficients which are a nondimensional representation of the integrated air load, and from which numerical values of load in pounds can be obtained. The load coefficients were obtained from values of pressure coefficient by a process of mechanical and numerical integration. Plots of pressure distribution along rows A, B, C, D, and E (see fig. 5) were integrated mechanically to obtain longitudinal strip loads. These strip loads, in turn were integrated numerically over the horizontal and lateral projected areas of the canopies to obtain the vertical and side load components, respectively. These load components were then nondimensionalized by dividing by the cross-sectional area of the canopies taken normal to the plane of symmetry, thus giving the vertical and side force coefficients C_z and C_y.

RESULTS AND DISCUSSION

The experimental data obtained in the present tests are shown as pressure coefficients in figures 6 to 15 and as load coefficients in figures 16 and 17. Before discussing the load-coefficient data, it is convenient first to present the external-pressure-coefficient data on the front and rear canopies, then the data on the internal-pressure coefficients for both canopies.

Pressure Distribution

The experimental-pressure-coefficient data for the front canopy are shown in figures 6 to 10 and for the rear canopy, in figures 11 to 15. Pressure distributions for the front and rear canopies at $\Psi = 0^\circ$ are given in figures 6 and 11, at $\Psi = -7.5^\circ$ in figures 7 and 12, and at $\Psi = 7.5^\circ$ in figures 8 and 13, respectively, for the different canopy positions tested. The results for $\Psi = 0^\circ$ are given at values of lift coefficient approximately equal to 0.17, 0.56, 0.98, and 1.33. The results for $\Psi = -7.5^\circ$ and 7.5° include data for the three higher values of C_L only, since flight tests at appreciable yaw angles in the high-speed flight condition were not considered feasible. Also shown are data obtained at $C_L = 1.33$ with the propeller idling. For each lift coefficient, the value of thrust coefficient at military power is based on figure 2. Data obtained in the check on the magnitude of distortion effects on the front canopy are shown in figure 9 and on the rear canopy in figure 14. The internal-pressure coefficient P_i for the front and rear canopy is plotted in figures 10 and 15, respectively, against lift coefficient with canopy position and yaw as parameters. The internal-pressure coefficients for both canopies are also given on the external-pressure-distribution plots for the various canopy positions, lift coefficients, and yaw conditions investigated.

The effects of the various parameters investigated on the external- and internal-pressure distributions for the front and rear canopies are summarized in the following discussion.

Front canopy.- With the front canopy closed, and at small values of thrust coefficient, the pressure distribution (fig. 6(a)) is essentially uniform from front to rear, but values of P_e at the sides are somewhat greater in magnitude than those at the top. Opening the canopy increases the magnitude of P_e over the forward part, but has little effect on the rearward part. The position of the rear canopy has negligible effect on the pressure distribution over the front canopy.

Yaw of the airplane introduces a component of flow normal to the plane of symmetry of the canopy the effects of which are illustrated by a comparison of figures 6(e), 7(d), and 8(d). The magnitude of P_e is increased over the top of the canopy and on the retarded side and is decreased on the advanced side. The effect of yaw is of about the same order of magnitude at both the front and rear of the canopy.

The effects of power on the front-canopy pressure distribution appear to be a resultant of effects introduced by the additonal longitudinal and rotational velocity components of the slipstream. Since these velocity components in general are proportional to T_c

and Q_c, respectively, the effects of power are more marked at slow speeds and thus in the present level-flight tests, at the higher values of C_L. As may be seen by a comparison of figures 6(e) and 6(d), which are for $\Psi = 0^\circ$ and the same lift coefficient, the additional velocity of the slipstream increases the magnitude of P_e, a little more so at the sides than at the top. In addition, the rotation of the slipstream introduces an asymmetry analogous to right yaw; that is, the left side becomes the advancing side, and increments due to power are smaller on the left side than on the right. As evidenced by the increment on the side of the canopy, the rotational effect is greater at the front than at the rear.

The combined effects of power and yaw are illustrated in figures 7(c) and 8(c). Asymmetry is marked in figure 8(c) since the effects of yaw to the right and slipstream rotation are in the same direction. The asymmetry is less marked for left yaw (fig. 7(c)) because the two effects are in opposite directions.

Although the changes of canopy pressure distribution associated with changes of lift coefficient are not completely defined by the present series of tests, an estimate of these changes at zero yaw can be obtained from a comparison of the data shown in figures 6(a) and 6(e), since power effects would be small in both cases. On the average, the increment in P_e due to a change in C_L of 1.16 appears to be greater than the increment associated with a change of T_c of 0.41.

Qualitative data on changes in load distribution due to distortion of the front canopy are shown in figure 9 for three positions of the front canopy. From the similarity of the pressure distributions shown in figure 9 for the two different load conditions, it is concluded that any changes in loading which might be ascribed to distortion of the front canopy are within the limits of the experimental error.

Rear canopy.— Because of the generally low level of pressures measured over the rear canopy, the scale of the values of external-pressure coefficient plotted in figures 11 to 14 has been expanded. This fact should be borne in mind when comparing the results with front-canopy plots. The data shown in figures 11 to 13 are for flights at the same conditions as the corresponding figures for the front canopy (figs. 6 to 8). Data for the external-pressure coefficient P_e are shown, however, for only two canopy positions — front open, rear open and front open, rear closed. A preliminary examination revealed that these two positions represented the maximum and minimum values of external load.

The effects of power, yaw, and lift coefficient on the rear-canopy pressure distribution are similar to those on the front canopy, but the effects of power and C_L appear to be of lesser magnitude. The position of the front canopy had a negligible effect on the pressure distribution over the rear canopy. The deflectors which extend into the slipstream when the rear canopy is open have a marked local effect on the canopy pressure distribution, as may be noted in figure 11. The blocking action of the extended deflectors is evident at stations 16 and 19 ahead of the deflector, while immediately behind the deflectors high values of negative pressure coefficient are observed.

From the similarity of the pressure distributions shown in figure 14 for the two different load conditions, it is concluded that any changes in loading which might be ascribed to distortion of the rear canopy are within the limits of the experimental error.

Internal pressure.- In general, the internal canopy pressures (figs. 10 and 15) were found to depend on the pressure field over the airplane and the area and location of any openings between the interior and exterior. With both canopies closed, the values of P_i in both cockpits indicate a pressure slightly less than free stream. Since there is no effective partition between the two cockpits, internal pressure on the front and rear canopies is essentially the same. Opening the front canopy with the rear closed reduced the rear internal pressure more than opening the rear canopy with the front canopy closed reduced the front internal pressure. This result is in accord with the observed magnitudes of the external pressures over the two canopies. Similarly, with either canopy partly or fully open the effects of yaw and power on P_i show a close correlation with their effects on P_e.

Comparison with wind-tunnel tests.- The flight data illustrated in figures 6 to 15 for an altitude of 8000 feet do not cover the full range of flight conditions simulated in the full-scale-tunnel tests especially with respect to thrust and torque coefficients. Comparison of figures 6 to 15 with the figures of reference 2 shows good qualitative agreement, however, and confirms the principal conclusions of reference 2 as to the effects of canopy position, yaw, power, and lift coefficient on the external- and internal-pressure distributions for the front and rear canopies.

Load Coefficient

Data on the integrated air loads expressed in coefficient form are given for the front canopy in figure 16 and for the rear canopy in figure 17. These load coefficients express quantitatively the effects of C_L, power, canopy position, and yaw discussed under the section

entitled "Pressure Distribution." The data shown are applicable to the present airplane operating with propeller idling or at military power in level flight at an altitude of 8000 feet. Numerically different results would be obtained at other altitudes or power settings or at other load factors, since the thrust–torque–lift relationships shown in figure 2 would not apply. For convenience, the load–coefficient data have been plotted against C_L, since the effects of slipstream longitudinal and rotational velocity components could not be completely separated in the present abbreviated flight program. Since, however, any increment in load coefficient due to power would be practically negligible at $C_L = 0.17$, an estimate of the relative magnitude of power effects as compared to lift–coefficient effect can be obtained by comparing the data at $C_L = 0.17$ with the propeller idling and the military–power data ($T_c = 0.43$) at $C_L = 1.33$.

The vertical load coefficients C_{z_e} and C_{z_i} for the front and rear canopies are presented in figures 16(a), 16(e), 17(a), and 17(e). The lateral load coefficients on the right and left sides of the canopy $C_{y_{e_R}}$ and $C_{y_{e_L}}$ are given in figures 16(b), 16(c), 17(b), and 17(c). The net lateral load coefficients C_y equal to the difference $C_{y_{e_L}} - C_{y_{e_R}}$, are shown in figures 16(d) and 17(d). Positive values of C_y indicate a net force to the left. The internal lateral load coefficient C_{y_i} which differs from C_{z_i} only by a numerical factor is shown on the auxiliary ordinate of figures 16(e) and 17(e).

External and internal load coefficients are given rather than net load coefficients in order that the results may be extended to other similar configurations for which the internal pressures may be markedly different. The effects of the various parameters investigated on the internal cockpit pressure discussed for the present case under the section entitled "Pressure Distribution", apply also to the internal load coefficients C_{z_i} and C_{y_i}. The internal load coefficients are presented, therefore, in order to determine readily whether the net vertical load coefficient, ($C_z = C_{z_e} - C_{z_i}$) or the net lateral load coefficient on either the left or right side of the canopy is, for the present case, in an exploding or in a crushing direction.

Front canopy.– The load–coefficient data presented for the front canopy at zero yaw indicate that C_{z_e}, $C_{y_{e_R}}$, and $C_{y_{e_L}}$ (figs. 16(a) to 16(c)) increase with both C_L and power; whereas the change of C_y

(fig. 16(d)) with power was more marked than the change with C_L. For the six different canopy positions investigated the upper limits of the external load coefficients presented for various values of C_L occur for the front canopy 3 inches and one-half open; the lower limits occur for the front canopy open and closed. Lines have been faired through the data for those limiting conditions. The effect of rear-canopy position on the front-canopy external load coefficients was negligible.

The incremental value of the external vertical and lateral load coefficients shown in figure 16 for $C_L = 1.33$ at idling power indicate that the effect of yaw of 7.5° on the front-canopy load coefficients, in general, was small. The combined effect of power and yaw, however, was marked. Yaw to the right generally produced higher values of C_{Z_e} than did yaw to the left, and the increment due to yaw was nearly independent of lift coefficient. The lateral load coefficients on the advancing side were decreased in general by approximately the same amount as the increase on the retarded side; $\Delta C_{y_{e_R}}$ with right yaw was, however, generally larger than was $\Delta C_{y_{e_L}}$ with left yaw, as shown by the results for the lateral-load-coefficient increment ΔC_y. Although the incremental load coefficients due to yaw show variations with canopy position, a detailed analysis is not considered warranted. The curves shown have been faired through the average values.

Examination of the load-coefficient data presented for the front canopy shows that the highest net loads for the present case occurred in the high-speed flight condition with the front and rear canopies closed and were in the exploding direction.

Rear canopy.- The load-coefficient data presented for the two rear canopy positions indicates that the external load coefficients C_{Z_e}, $C_{y_{e_R}}$, and $C_{y_{e_L}}$ (figs. 17(a) to 17(c)) are not only smaller than the front-canopy coefficient but also show a comparatively smaller variation with C_L and power.

For the rear-canopy open position, values of C_{Z_e}, $C_{y_{e_R}}$, and $C_{y_{e_L}}$ were higher at the idling power than at military power at $C_L = 1.33$. For the rear canopy closed, power increased the external load coefficients as in the case of the front canopy. For both canopy positions, the change in C_y with power was more marked than the change with C_L. At military power, the external load coefficients were essentially the same for both rear-canopy positions.

The effects of yaw of 7.5° on the external load coefficients for the rear canopy, shown by the incremental values in figure 17 for $C_L = 1.33$ at idling power, are small for the rear-canopy-closed position. For the rear canopy open, the effects of yaw on the vertical load coefficient C_{z_e} and the lateral load coefficients $C_{y_{e_R}}$ and $C_{y_{e_L}}$ were also small for the retarded side but the lateral load coefficients for the advancing side were markedly reduced.

The combined effect of yaw and power on the external load coefficient for the rear canopy was essentially the same as were noted for the front canopy. The value of $\Delta C_{y_{e_L}}$ (fig. 17(e)) for the rear-canopy-closed position, however, increased with right yaw, a result which is contrary to the general trend of left-lateral load-coefficient data, but which is consistent with the effects of power and yaw on the pressure distribution over the rear canopy as shown in figures 12 and 13.

The rear-canopy load-coefficient data for the present case indicate that the critical net load for the rear canopy occurred for the high-speed flight condition with the front canopy open and the rear canopy closed and was in the crushing direction. Local crushing loads on the left side of the canopy produced by the combined effect of the slipstream rotational velocity at military power and the asymmetric air flow due to yaw were higher than the average net canopy loads.

CONCLUSIONS

Results from a flight investigation conducted to obtain aerodynamic loading and pressure-distribution data on the conventional front and rear sliding canopies showed that for the range of conditions investigated:

1. The highest net loads for the front canopy were in the exploding direction and occurred with the front and rear canopies closed.

2. The highest net loads for the rear canopy were in the crushing direction and occurred with front canopy open and rear canopy closed.

3. The combined effect of the slipstream rotational velocity at military power and the asymmetrical air flow due to yaw produced net local exploding and crushing loads on both canopies that were higher than the average net canopy loads.

4. Changes in loading due to distortion of the front and rear canopies under load were within the limits of the experimental error for values of dynamic pressure up to approximately 50 percent of the value corresponding to the maximum permissible diving speed at sea level.

5. The flight data confirm the principal conclusions of the full-scale-tunnel tests as to the effect of canopy position, yaw, power, and lift coefficient on the pressure distribution over the front and rear canopies.

Langley Aeronautical Laboratory
National Advisory Committee for Aeronautics
Langley Air Force Base, Va.

REFERENCES

1. Cocke, Bennie W., Jr., and Czarnecki, K. R.: Canopy Loads Investigation for the F6F-3 Airplane. NACA RM L6L23a, 1947.

2. Dexter, Howard E., and Rickey, Edward A.: Investigation of the Loads on a Conventional Front and Rear Sliding Canopy. NACA RM L7D04, 1947.

3. Cocke, Bennie W., Jr.: Investigation of the Loads on a Typical Bubble-Type Canopy. NACA RM L7D07, 1947.

4. Matheny, Cloyce E., and Huston, Wilber B.: Flight Investigation of Loads on a Bubble-Type Canopy. NACA RM L8C30, 1948.

5. Danforth, Edward C. B., III, and Reeder, John P.: Flight Measurements of Internal Cockpit Pressures in Several Fighter-Type Airplanes. NACA TN 1173, 1947.

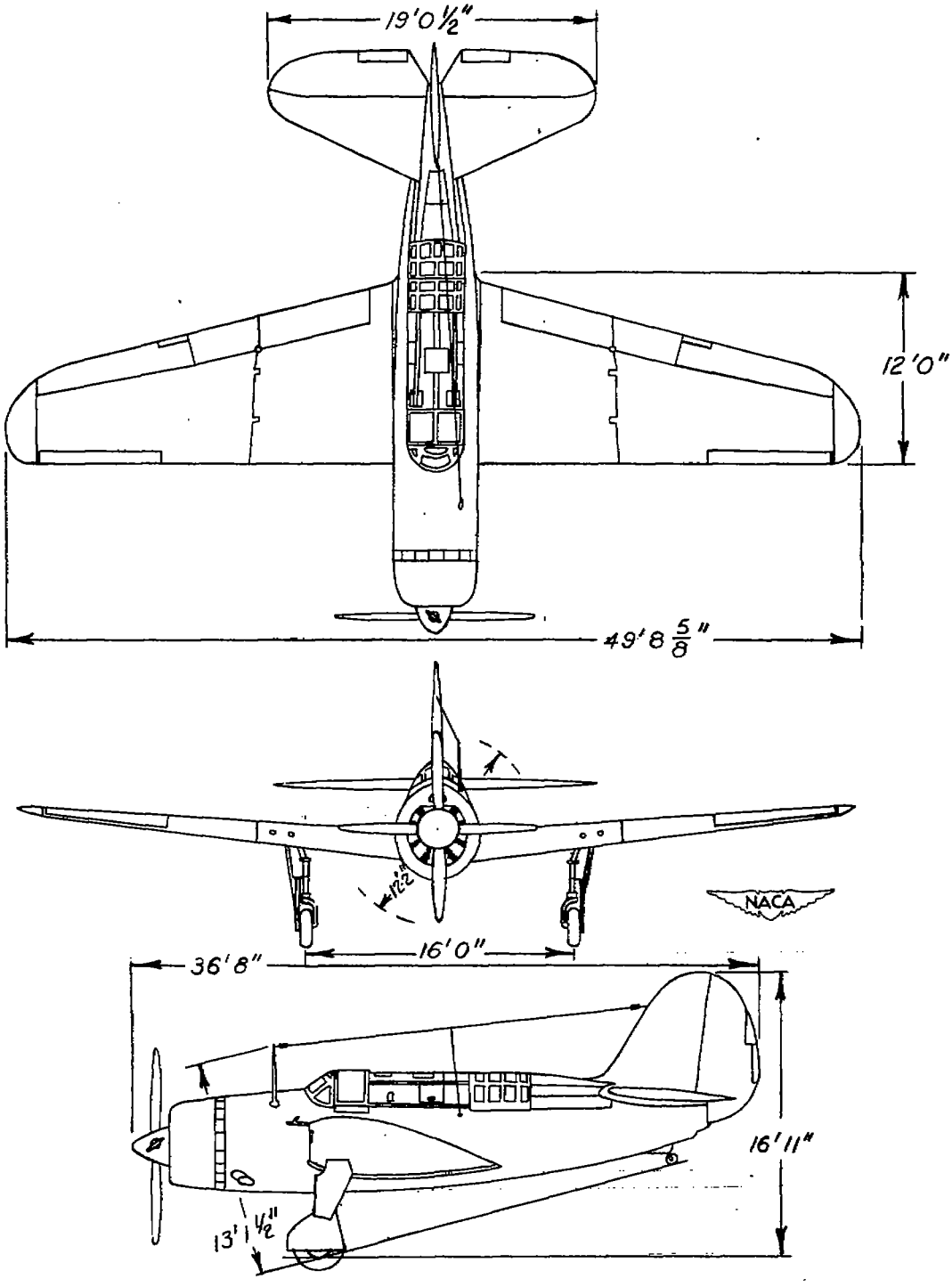

Figure 1.- The SB2C-4E airplane.

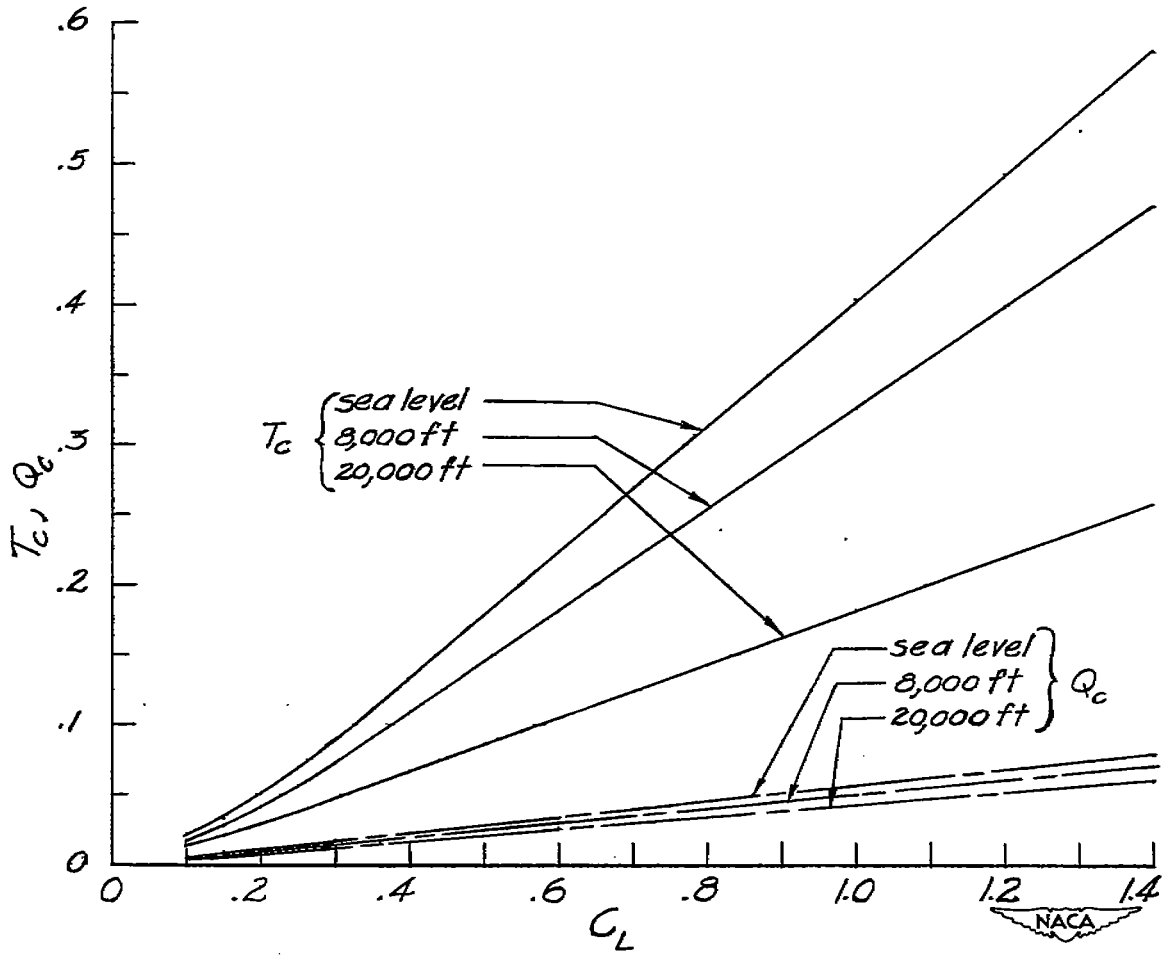

Figure 2.- Required thrust and torque coefficients for level flight at various altitudes.

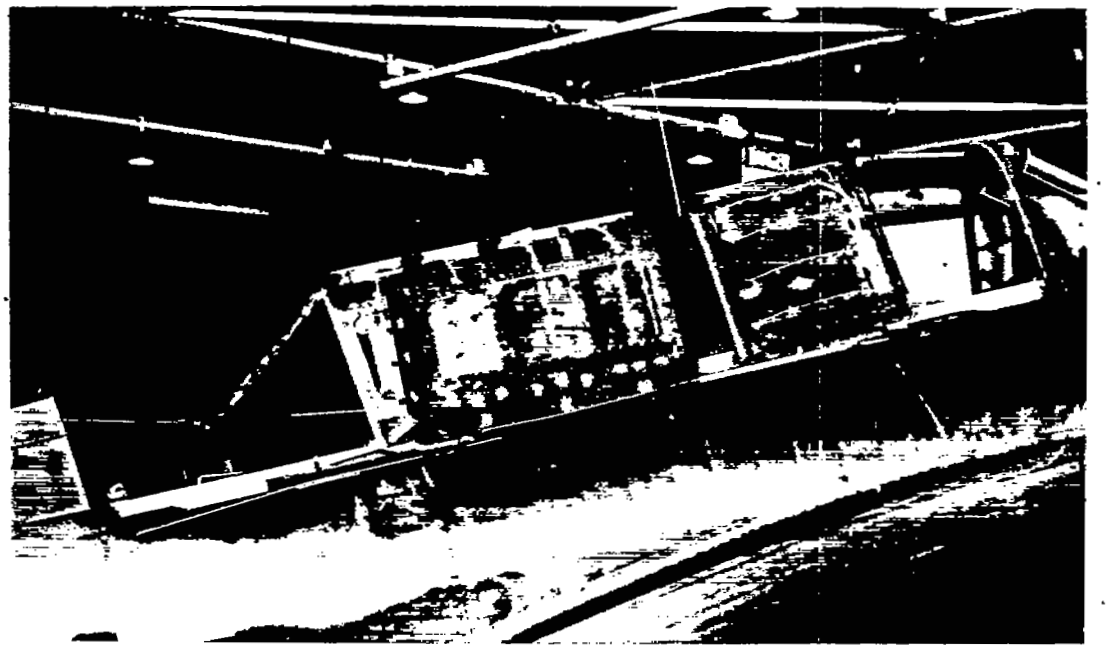

(a) Canopies open. NACA L-48699

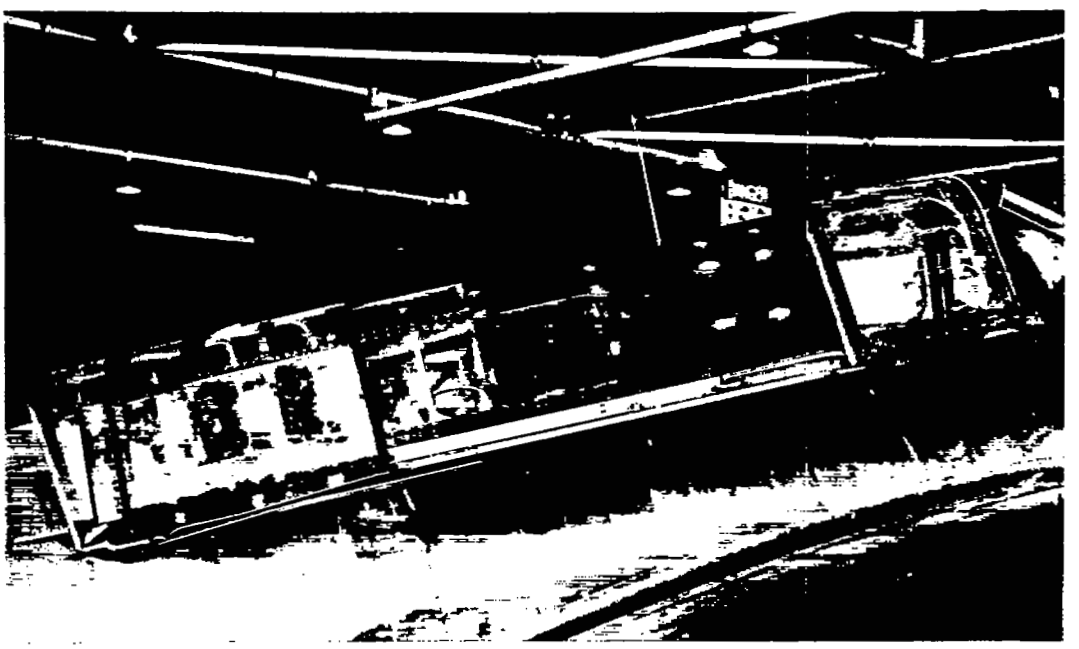

(b) Canopies closed. NACA L-48698

Figure 3.- The front and rear canopies in the open and closed positions.

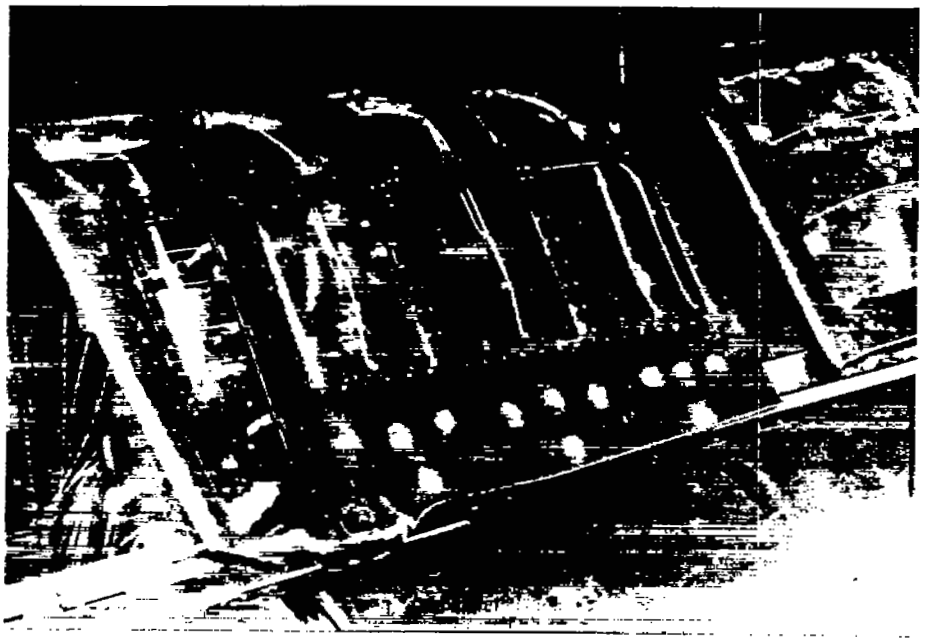

(a) Canopy and deflector open. NACA L-48700.1

(b) Canopy and deflector closed. NACA L-48701.1

Figure 4.- The rear canopy in the open and closed positions, showing the two positions of the deflectors.

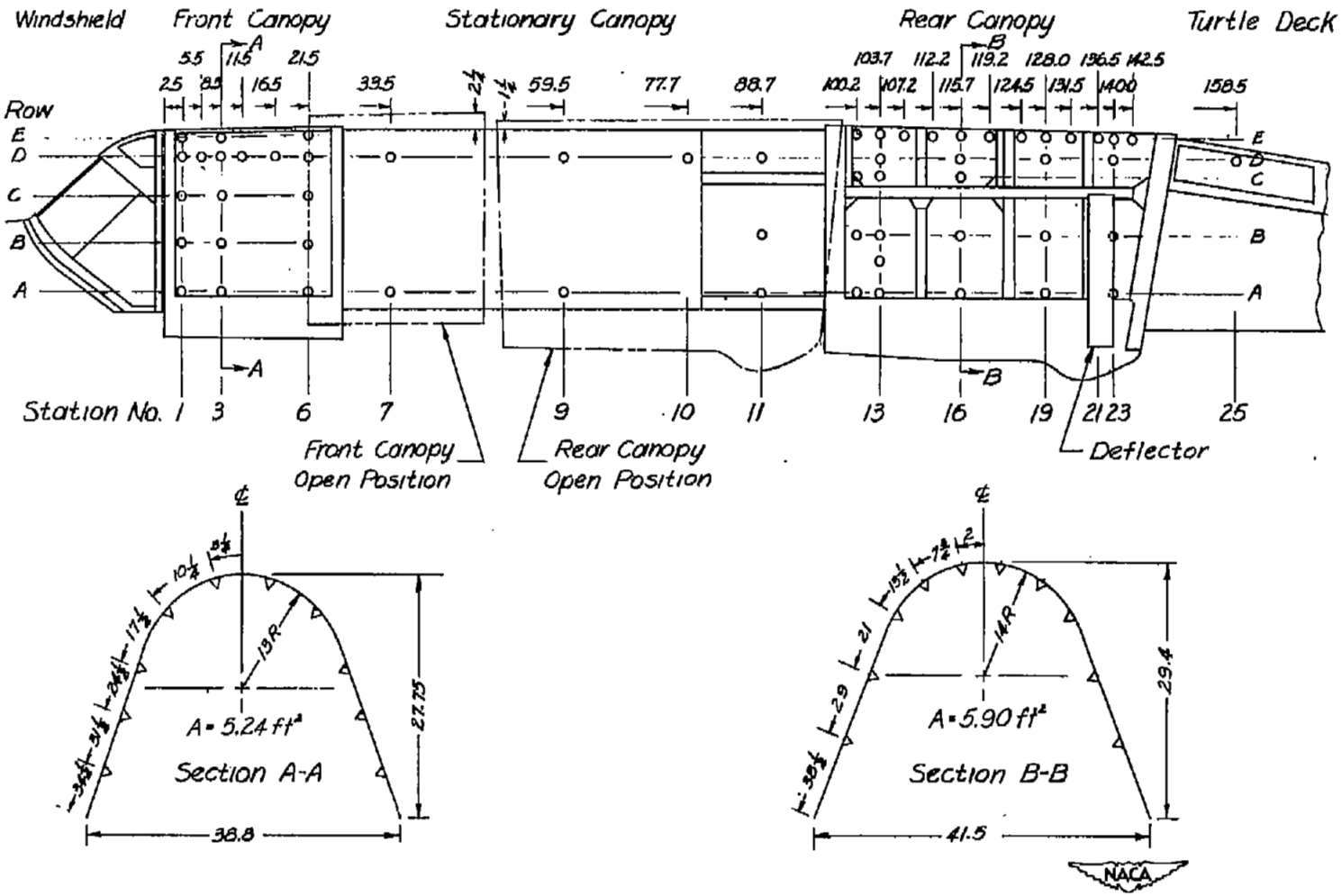

Figure 5.- Principal dimensions of the canopies and locations of the static-pressure orifices.

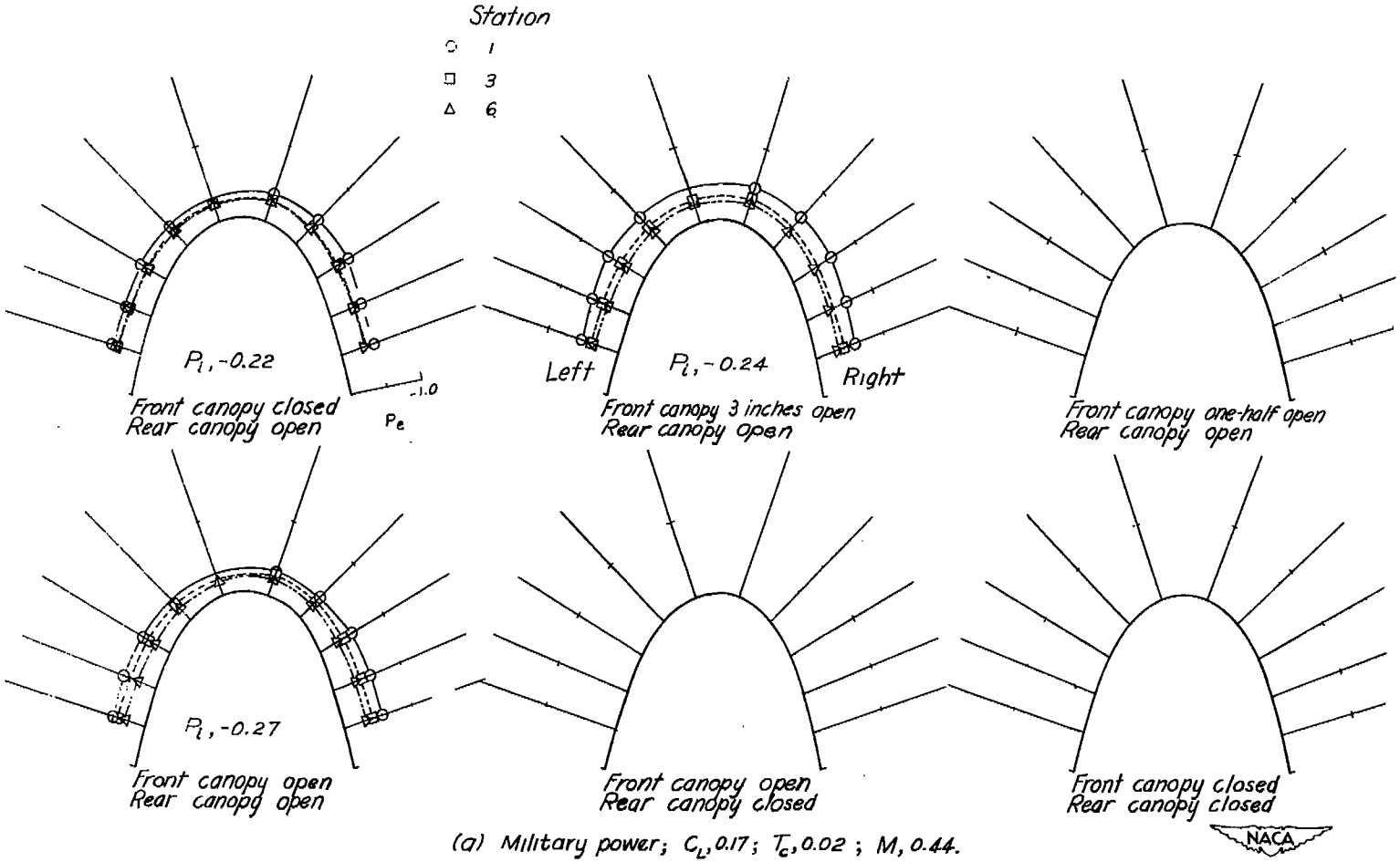

(a) Military power; C_L, 0.17; T_c, 0.02 ; M, 0.44.

Figure 6.- Pressure distributions over the front canopy of the SB2C-4E airplane. $\psi = 0^\circ$; $h_p = 8000$ feet.

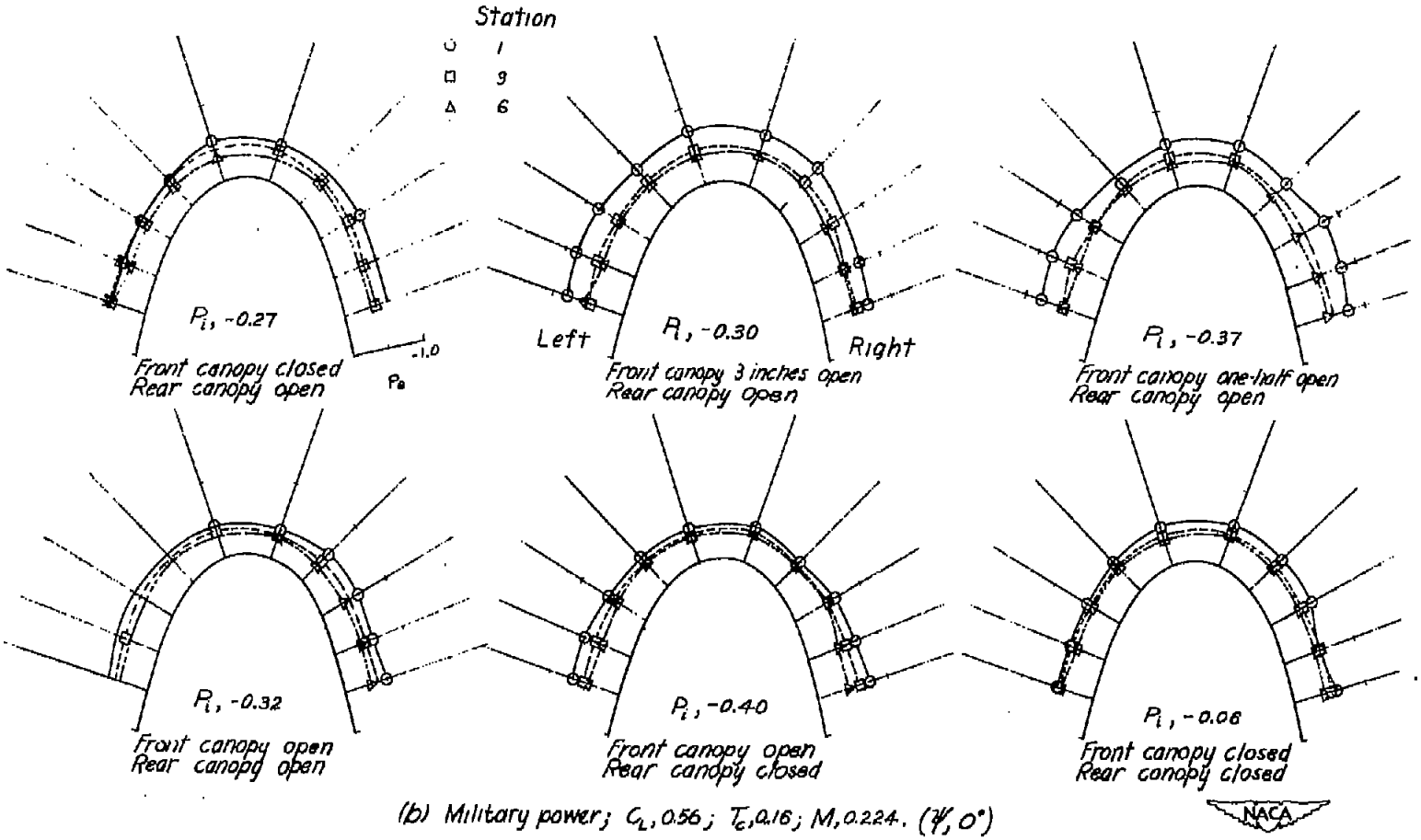

(b) Military power; C_L, 0.56; T_c, 0.16; M, 0.224. (Ψ, 0°)

Figure 6.- Continued.

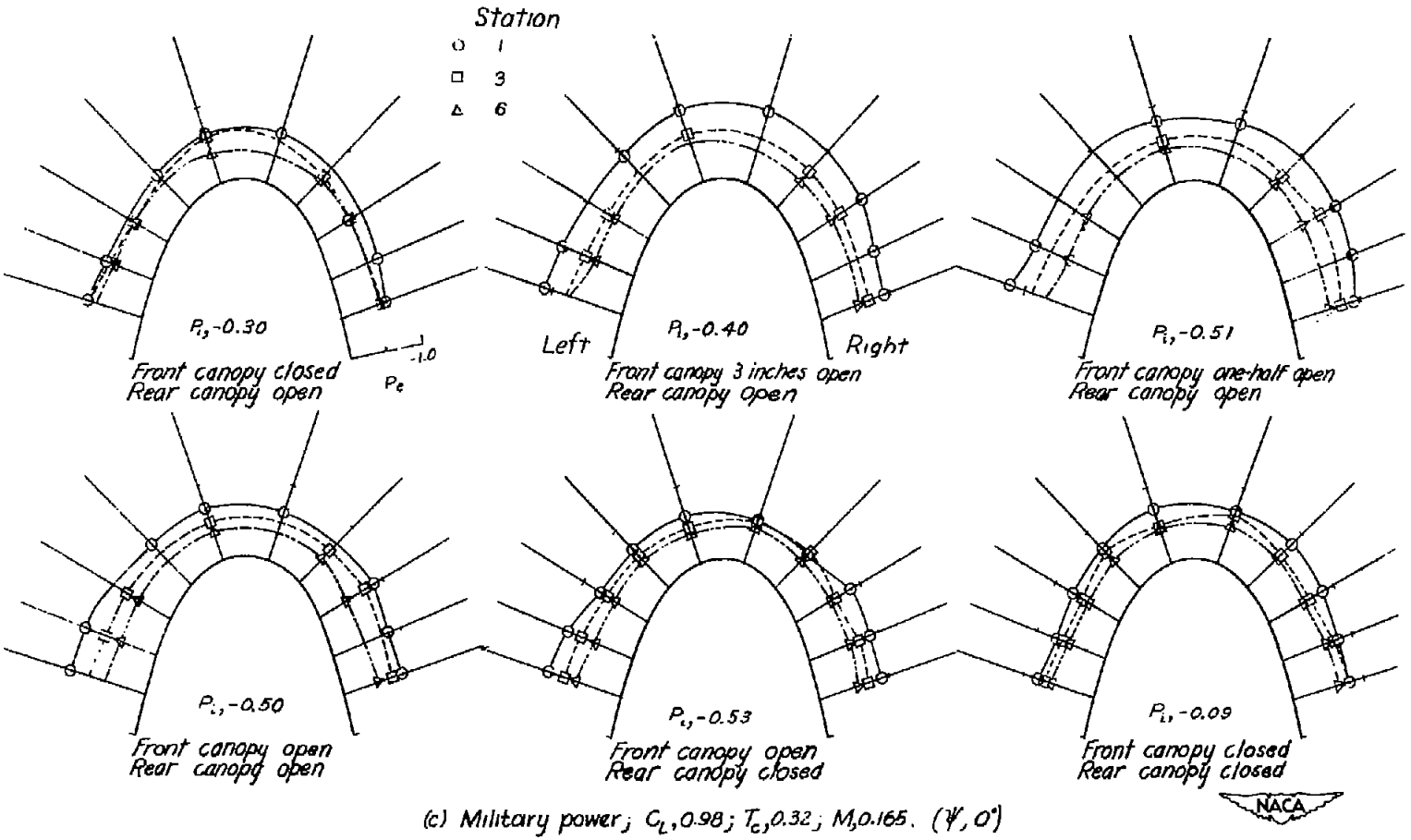

(c) Military power; C_L,0.98; T_c,0.32; M,0.165. (Ψ, 0°)

Figure 6.- Continued.

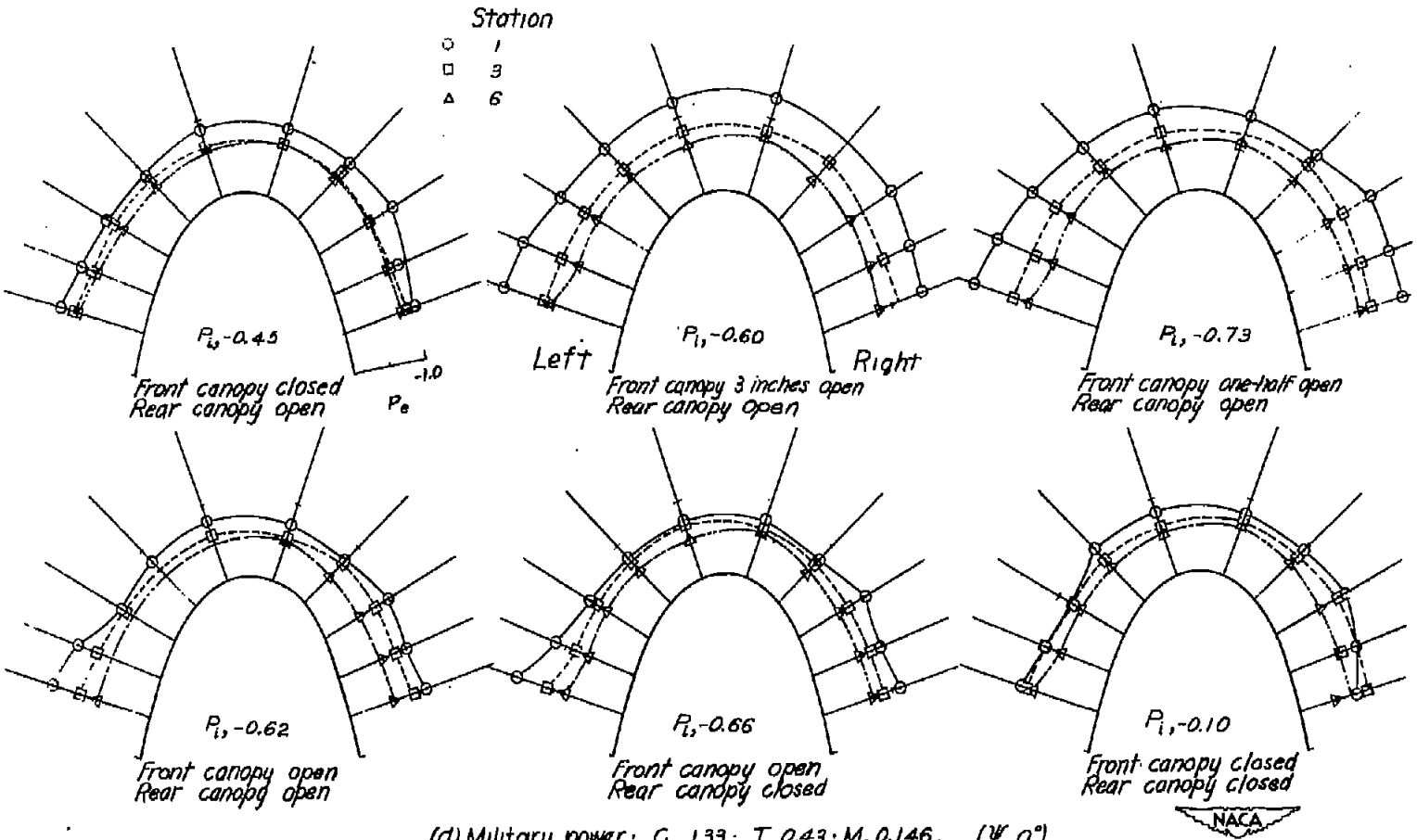

(d) Military power; C_L, 1.33; T_c, 0.43; M, 0.146. (Ψ, 0°)

Figure 6.- Continued.

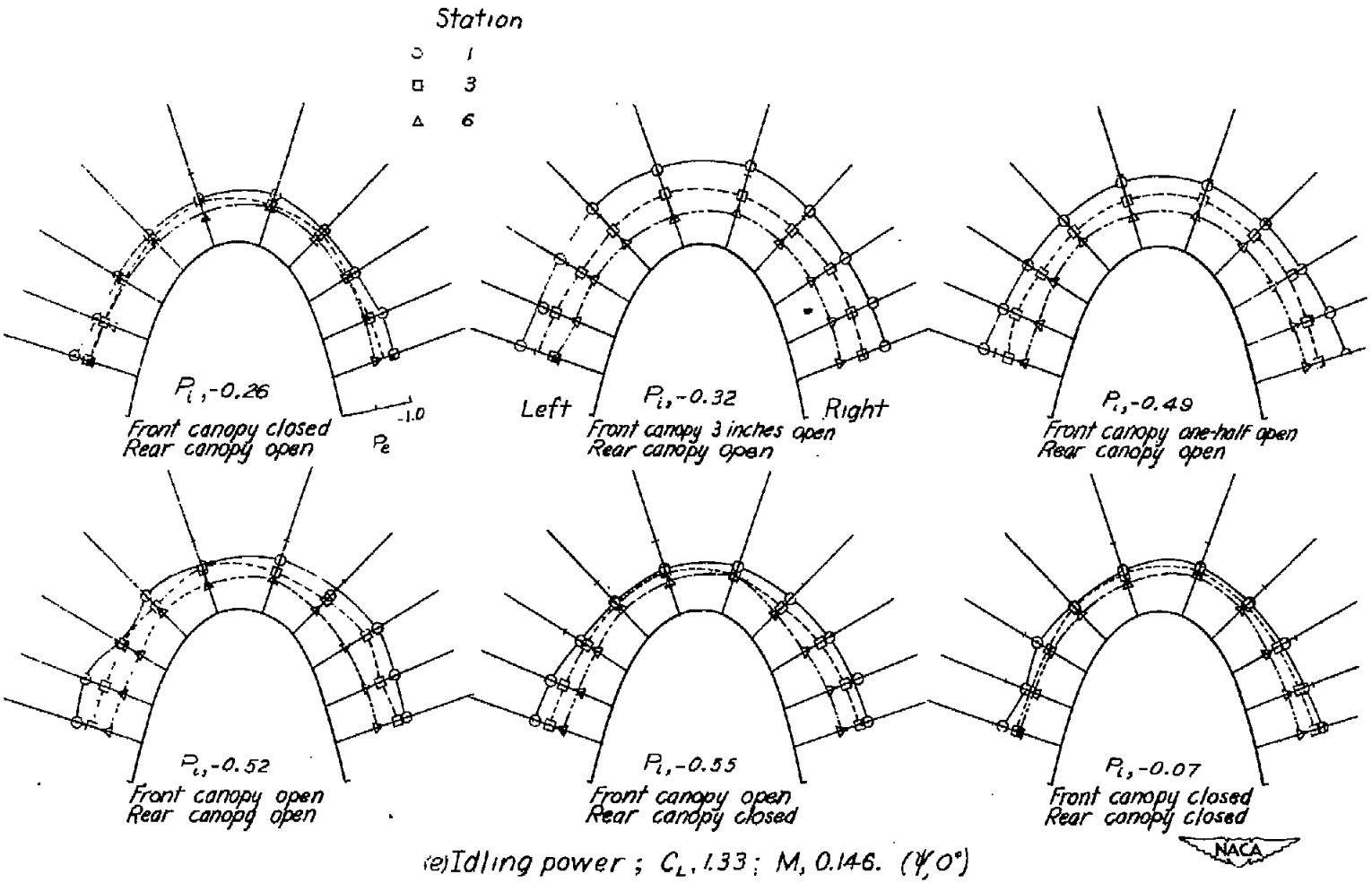

(e) Idling power; C_L, 1.33; M, 0.146. (Ψ, 0°)

Figure 6.- Concluded.

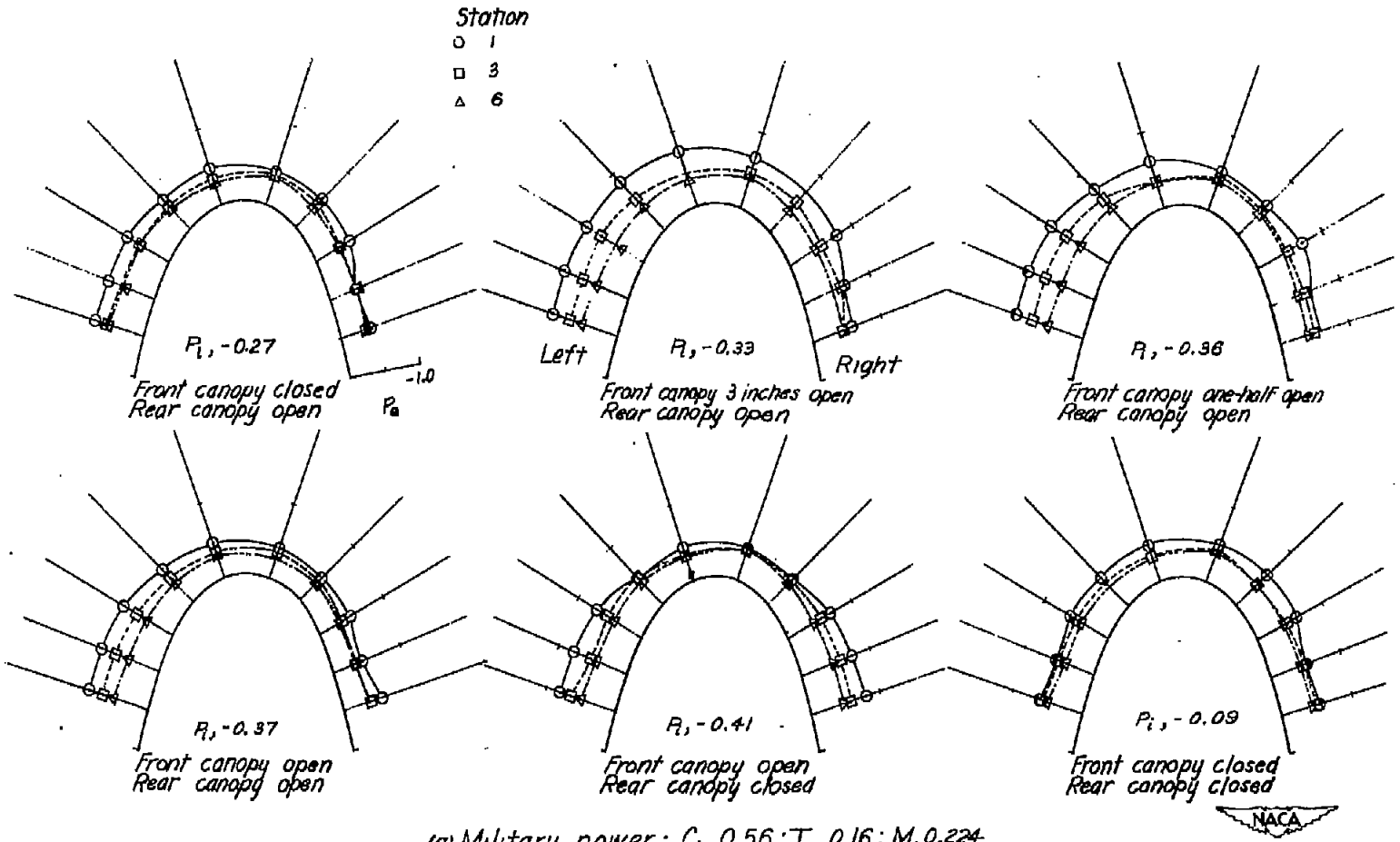

(a) Military power; C_L, 0.56; T_c, 0.16; M, 0.224.

Figure 7.- Pressure distributions over the front canopy of the SB2C-4E airplane. $\psi = -7.5^\circ$; $h_p = 8000$ feet.

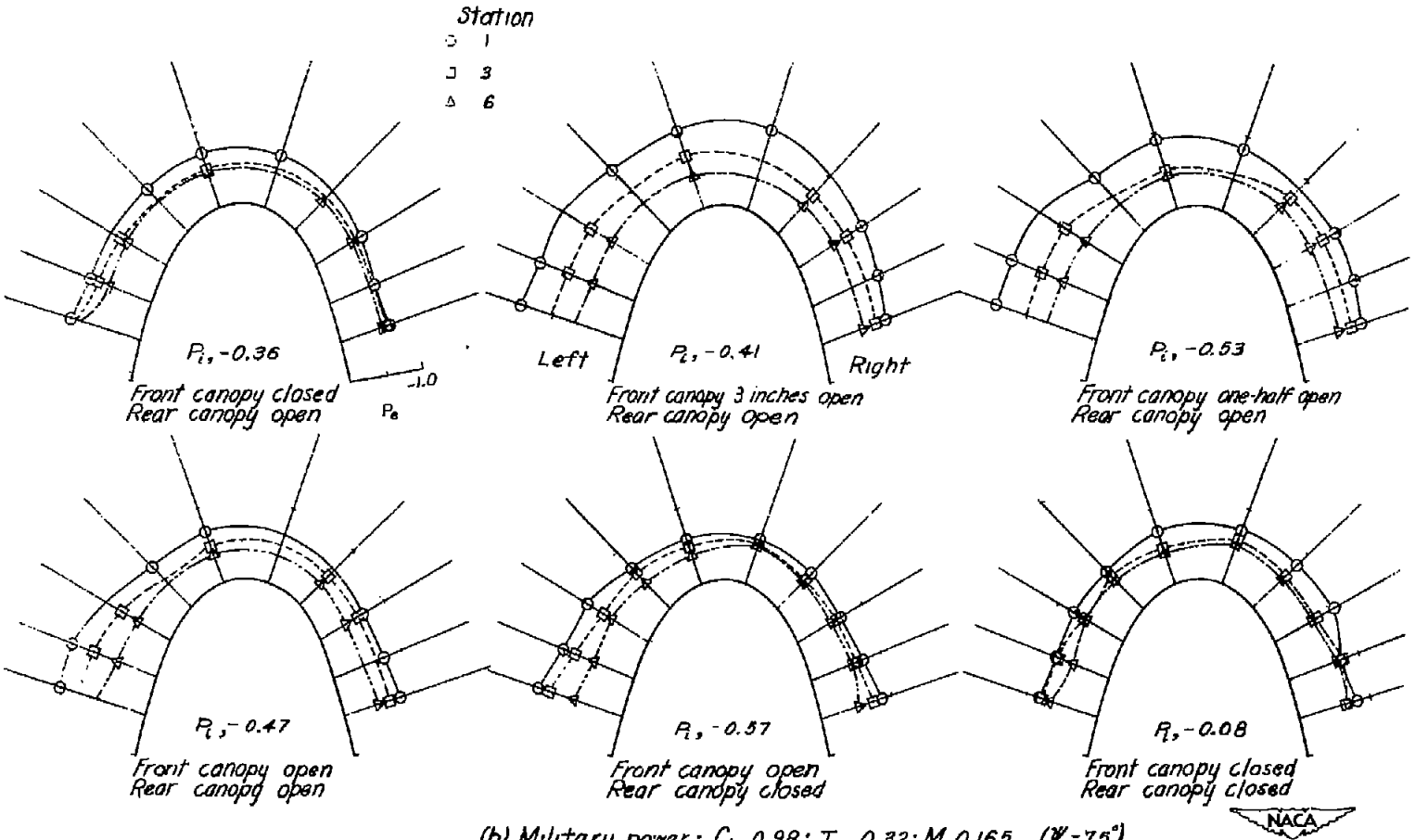

(b) Military power; C_L, 0.98; T_c, 0.32; M, 0.165. (γ, -7.5°)

Figure 7.- Continued.

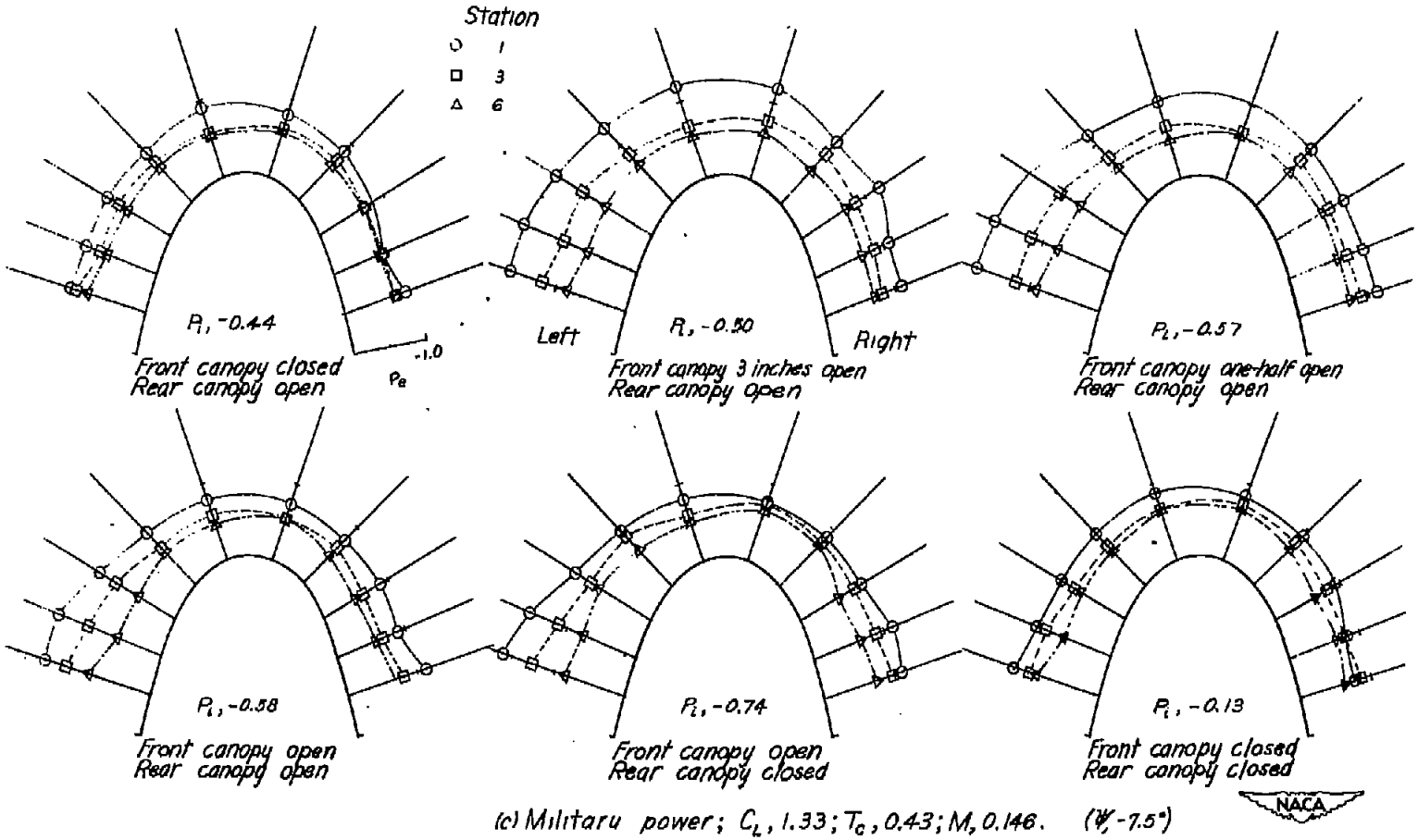

(c) Military power; C_L, 1.33; T_c, 0.43; M, 0.146. (Ψ, -7.5°)

Figure 7.- Continued.

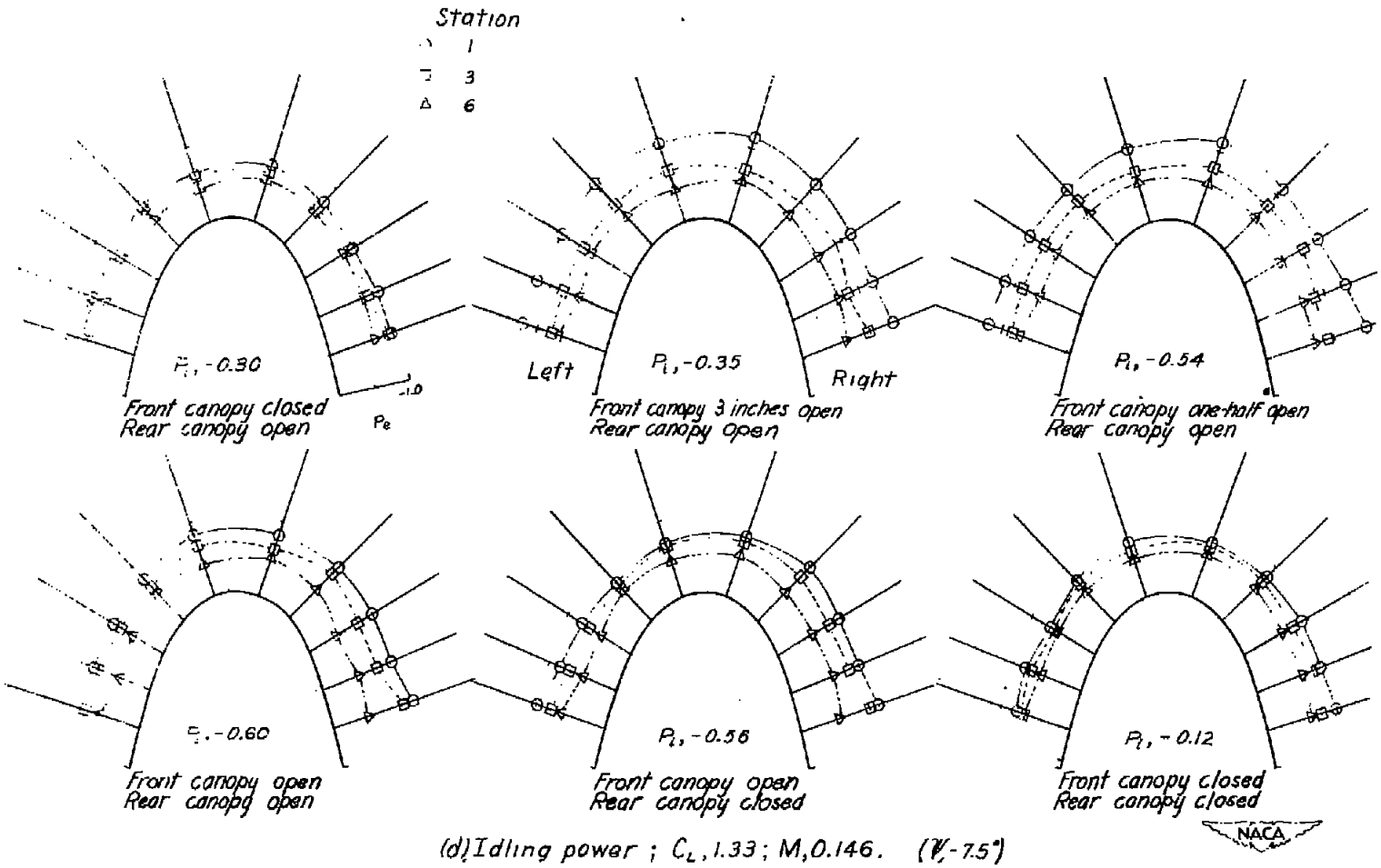

(d) Idling power ; C_L, 1.33 ; M, 0.146. (γ, -7.5°)

Figure 7.- Concluded.

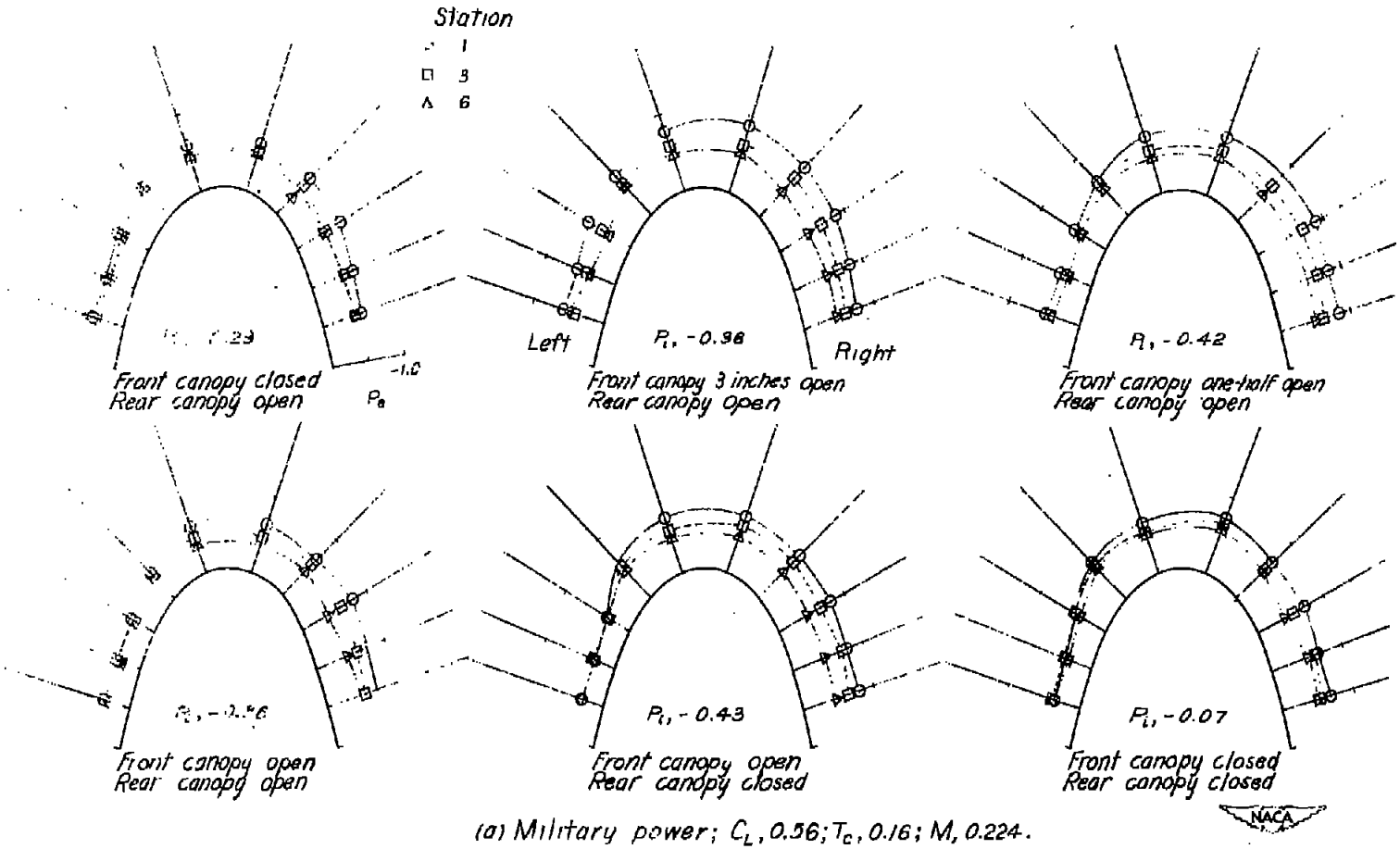

(a) Military power; C_L, 0.56; T_c, 0.16; M, 0.224.

Figure 8.- Pressure distributions over the front canopy of the SB2C-4E airplane. $\Psi = 7.5^\circ$; $h_p = 8000$ feet.

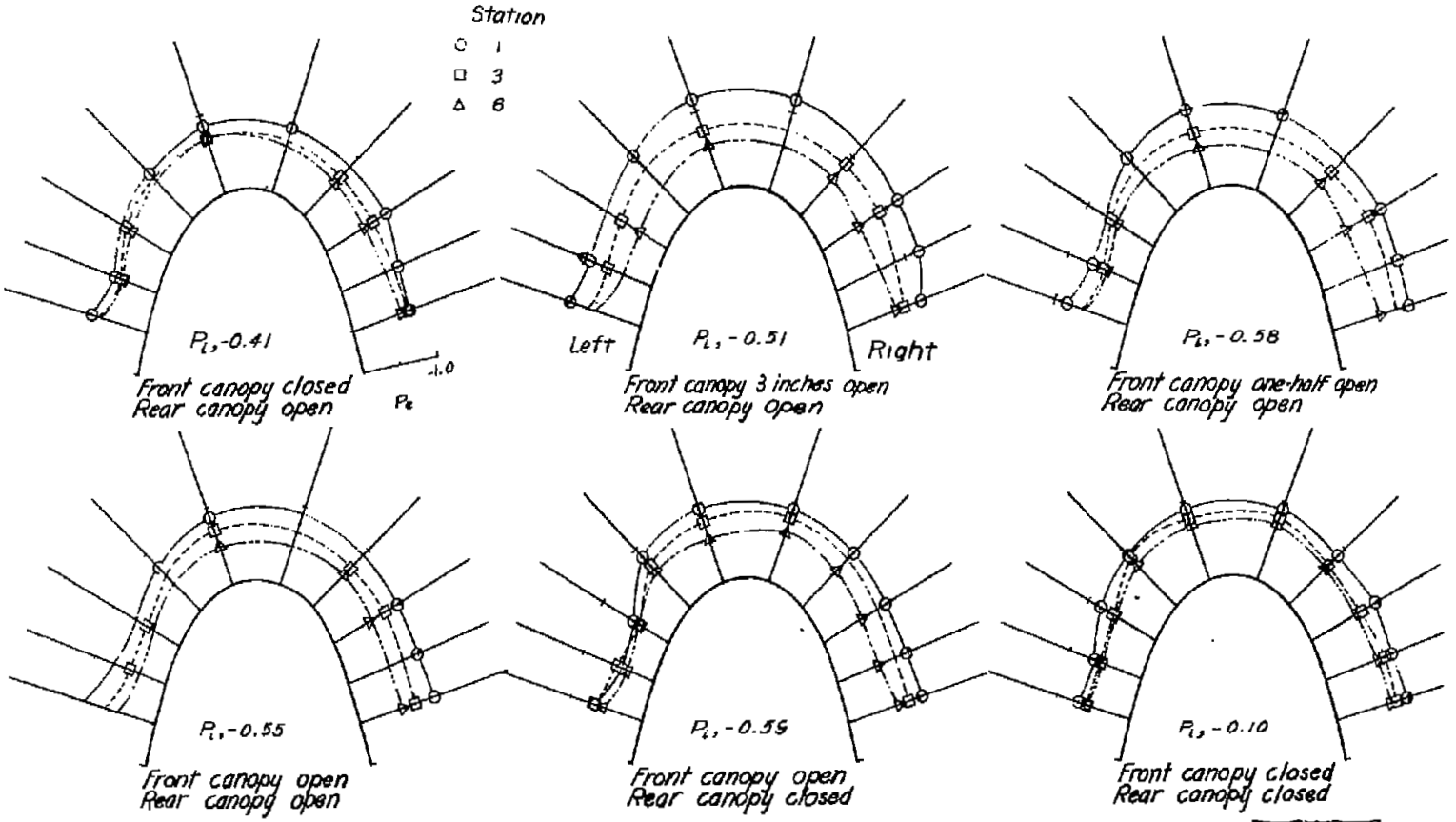

(b) Military power; C_L, 0.98; T_c, 0.32; M, 0.165. (γ, 7.5°)

Figure 8.- Continued.

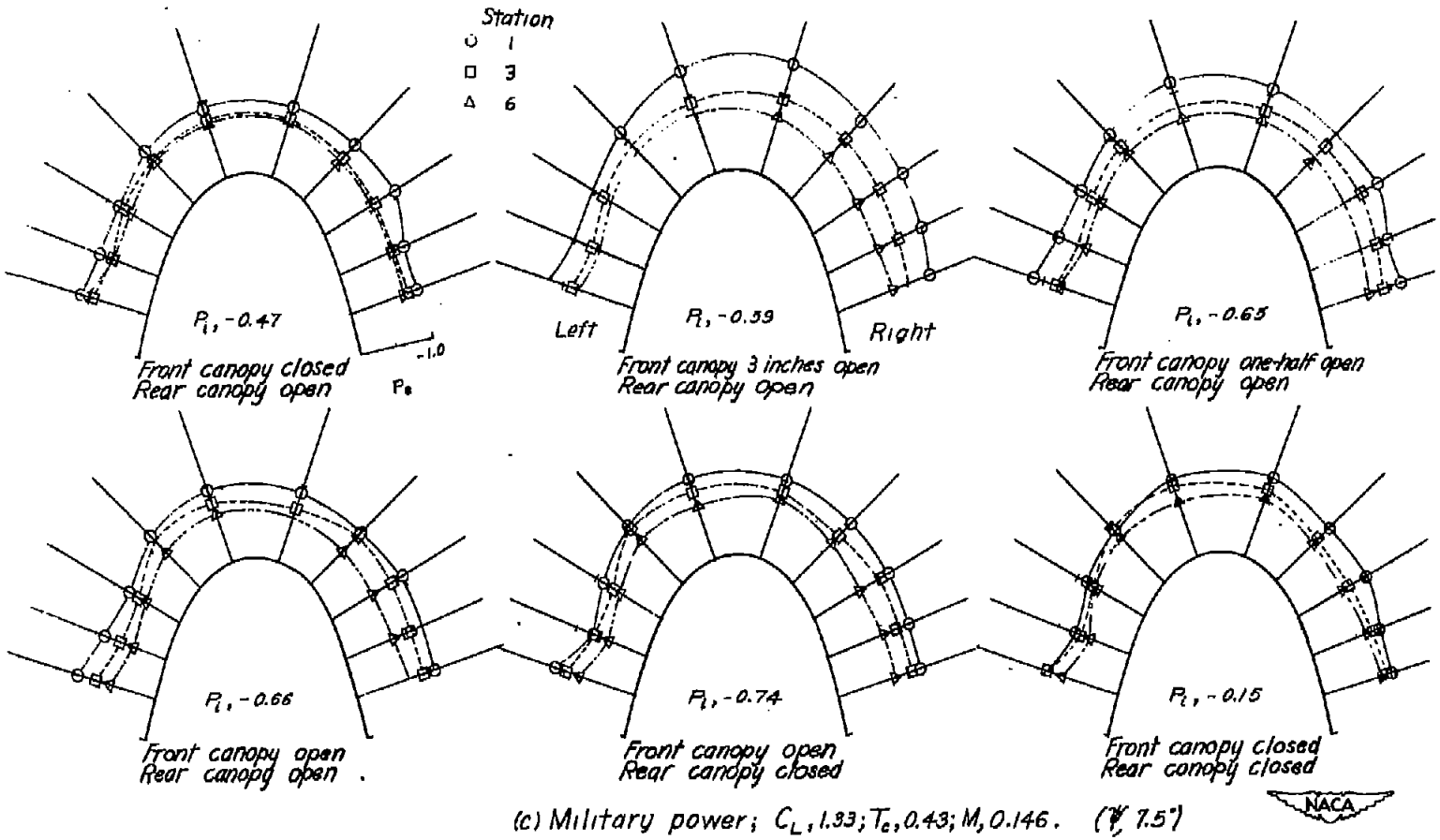

(c) Military power; C_L, 1.33; T_c, 0.43; M, 0.146. (i_t, 7.5°)

Figure 8.- Continued.

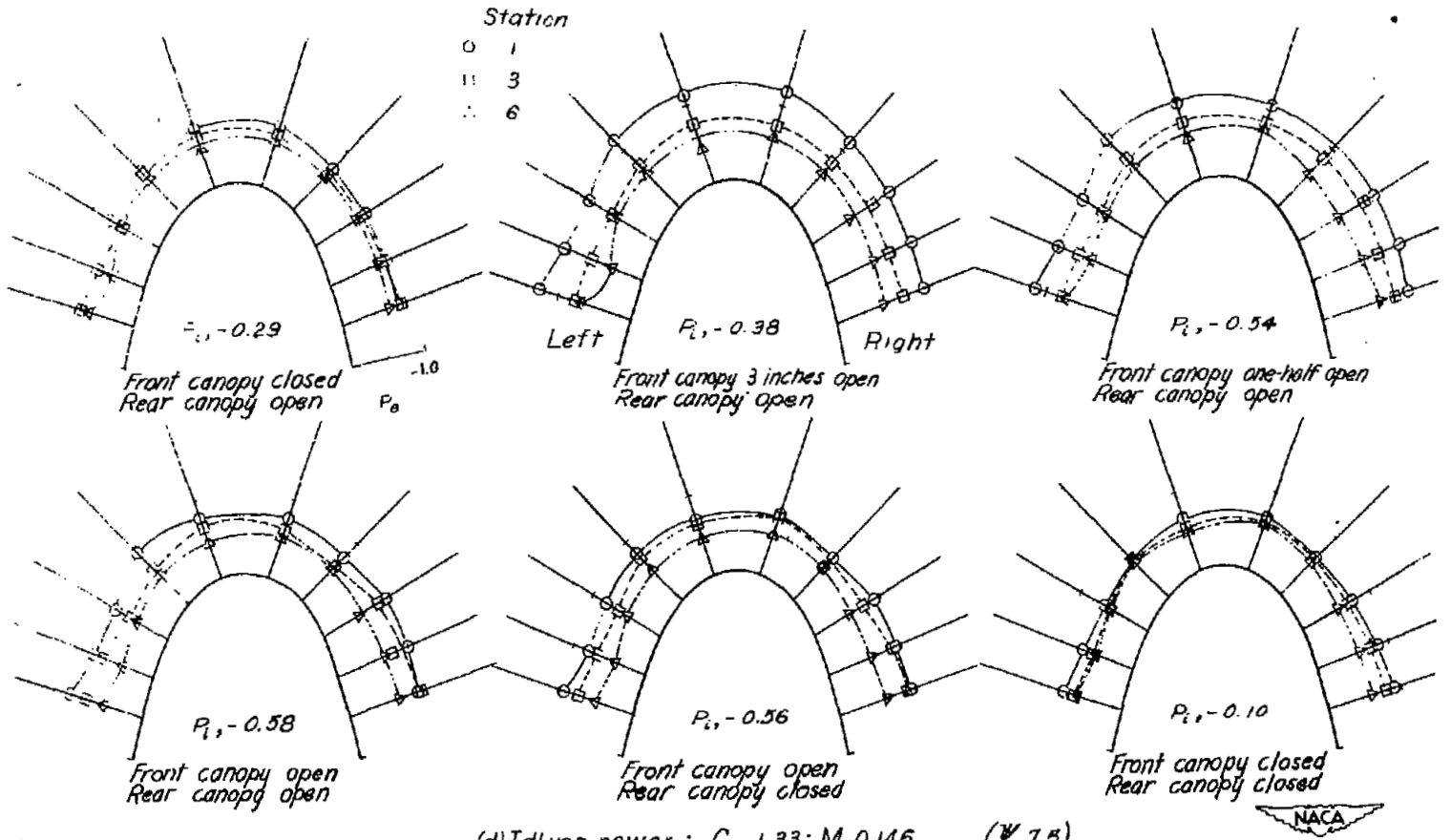

(d) Idling power ; C_L, 1.33; M, 0.146. (Ψ, 7.5)

Figure 8.- Concluded.

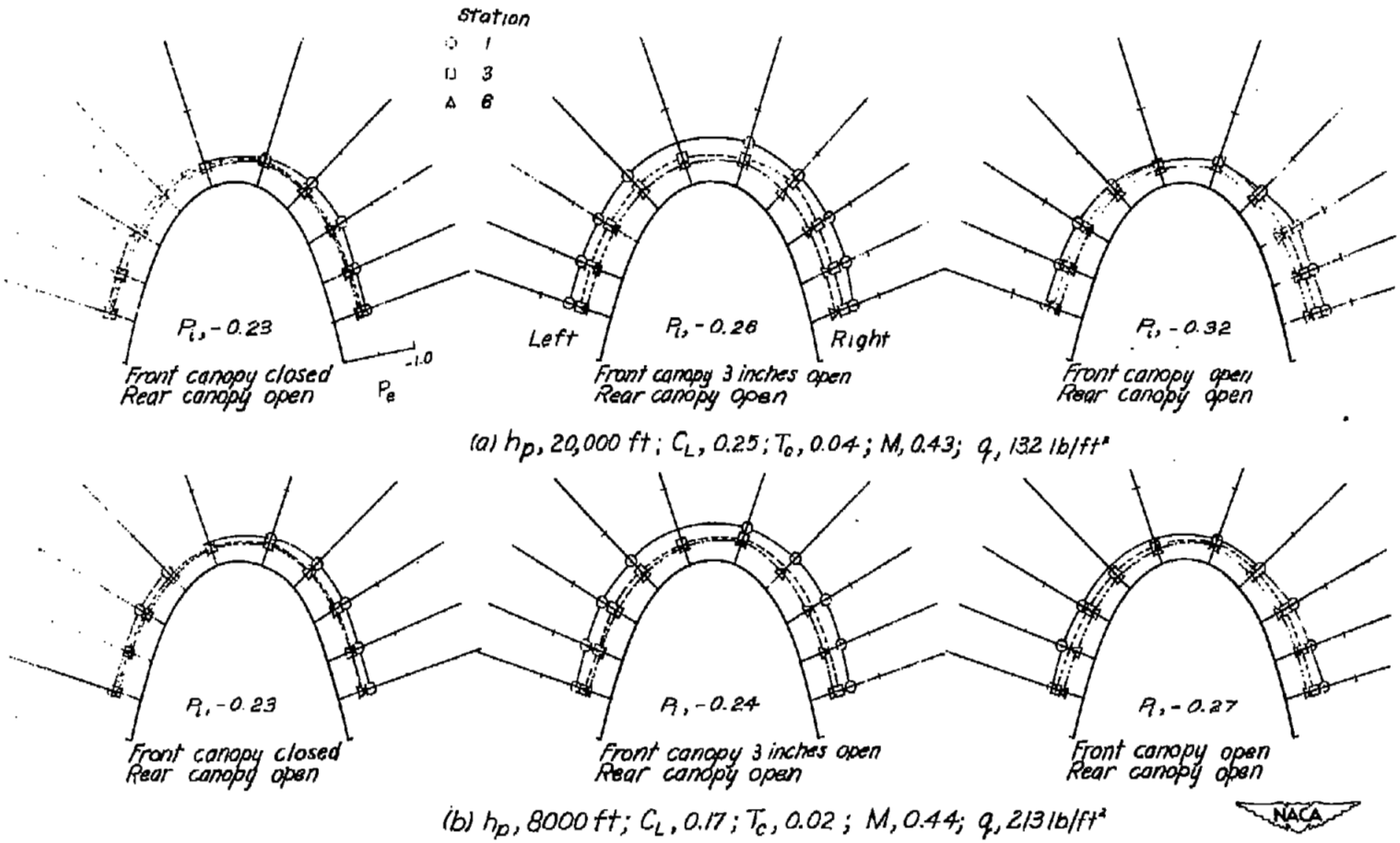

Figure 9.- Effect of distortion on the pressure distribution over the front canopy of the SB2C-4E airplane. $\Psi = 0^\circ$; military power.

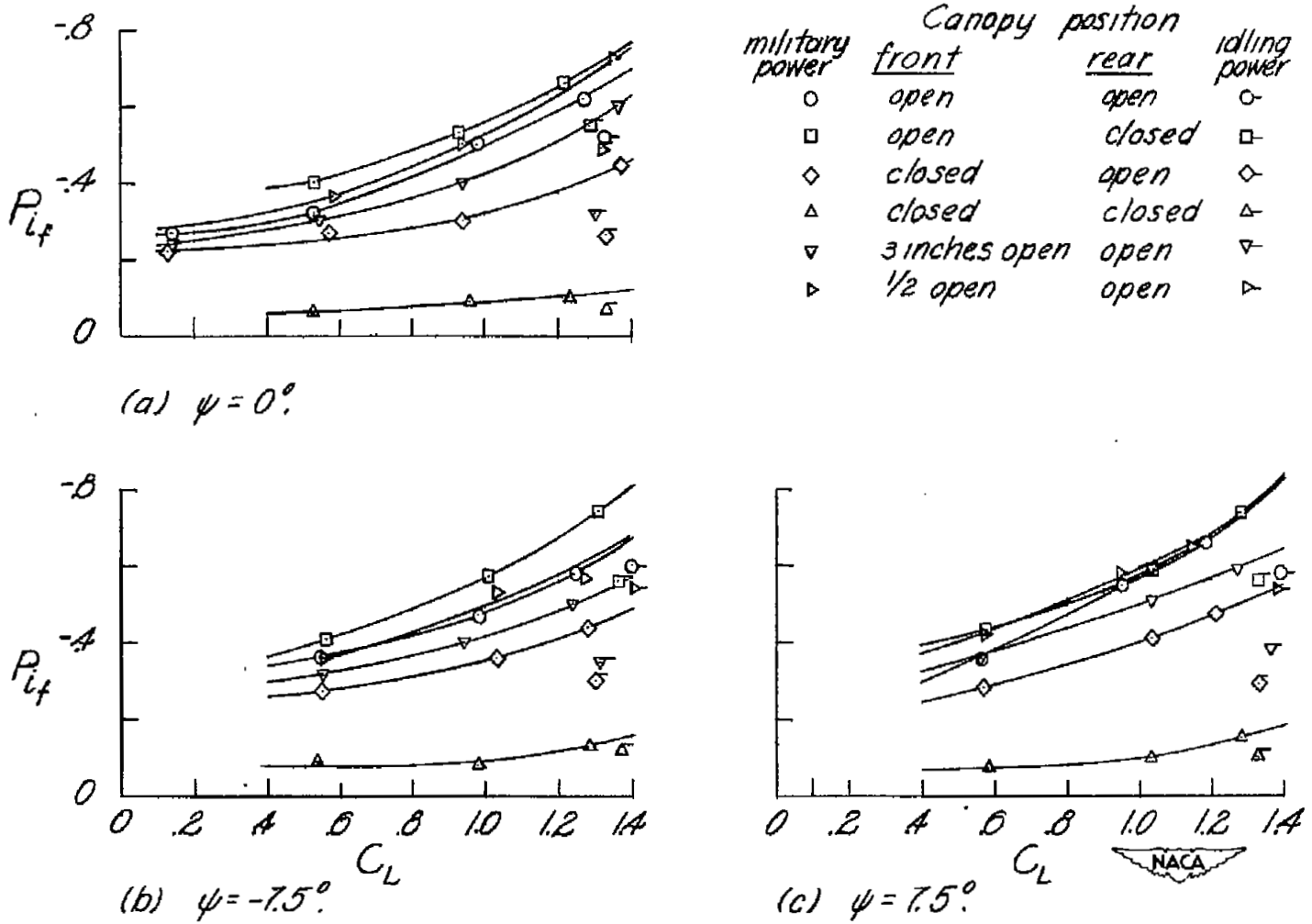

Figure 10.- Variation of front canopy internal pressure coefficient with lift coefficient for various yaw angles, canopy positions, and power settings.

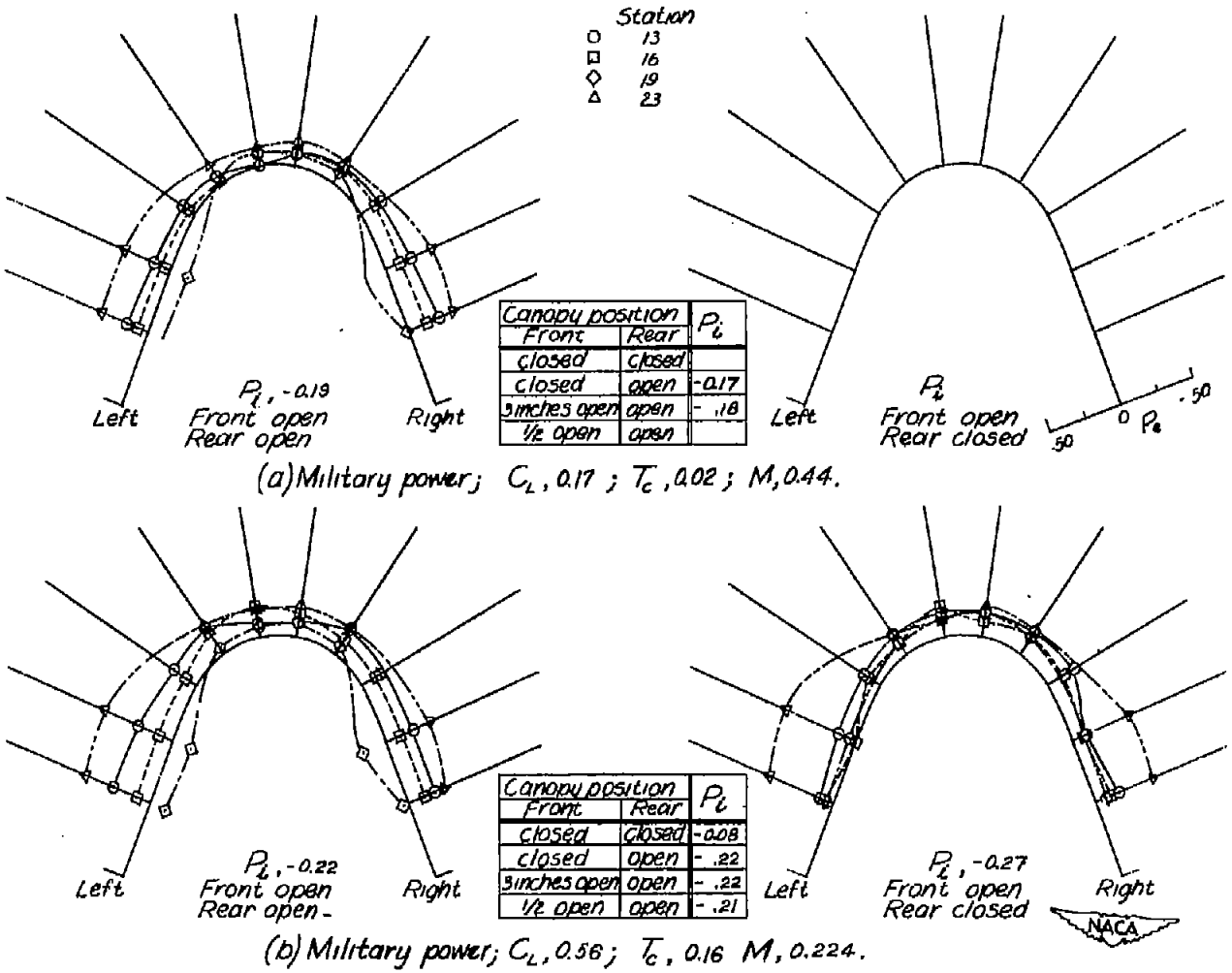

Figure 11.- Pressure distributions over the rear canopy of the SB2C-4E airplane. $\psi = 0^{\circ}$; $h_p = 8000$ feet.

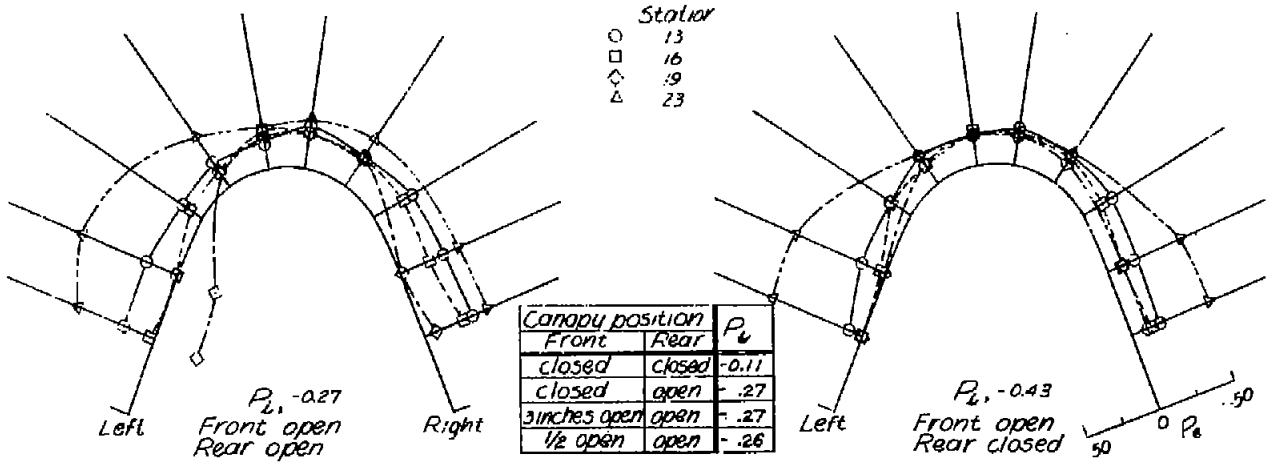

Canopy position		P_t
Front	Rear	
closed	closed	-0.11
closed	open	- .27
3 inches open	open	- .27
1/2 open	open	- .26

(c) Military power; C_L, 0.98 ; T_c, 0.32; M, 0.165. (Ψ, 0°)

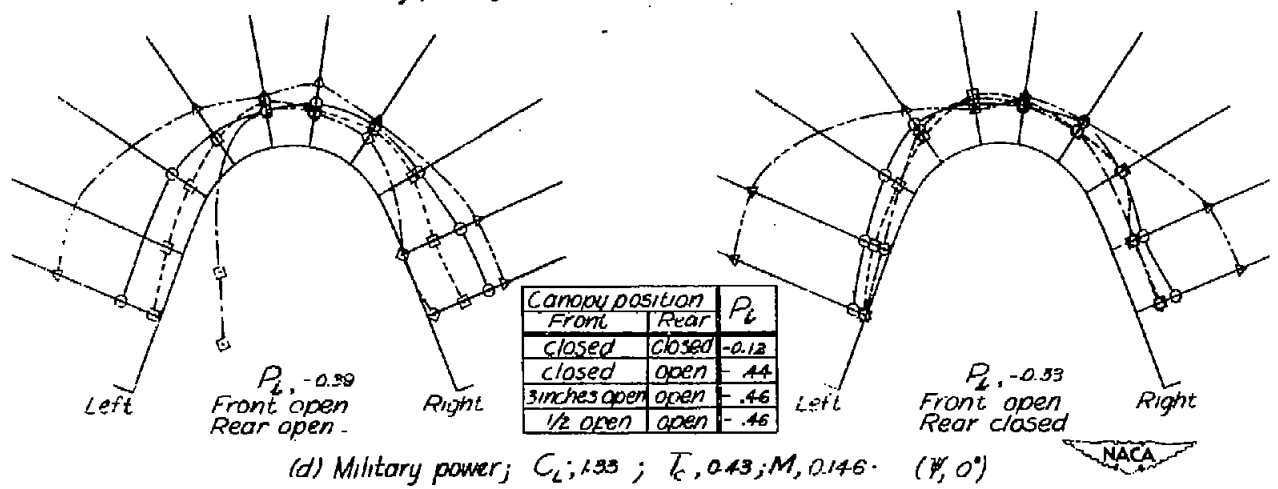

Canopy position		P_t
Front	Rear	
closed	closed	-0.12
closed	open	- .44
3 inches open	open	- .46
1/2 open	open	- .46

(d) Military power; C_L, 1.33 ; T_c, 0.43; M, 0.146. (Ψ, 0°)

Figure 11.- Continued.

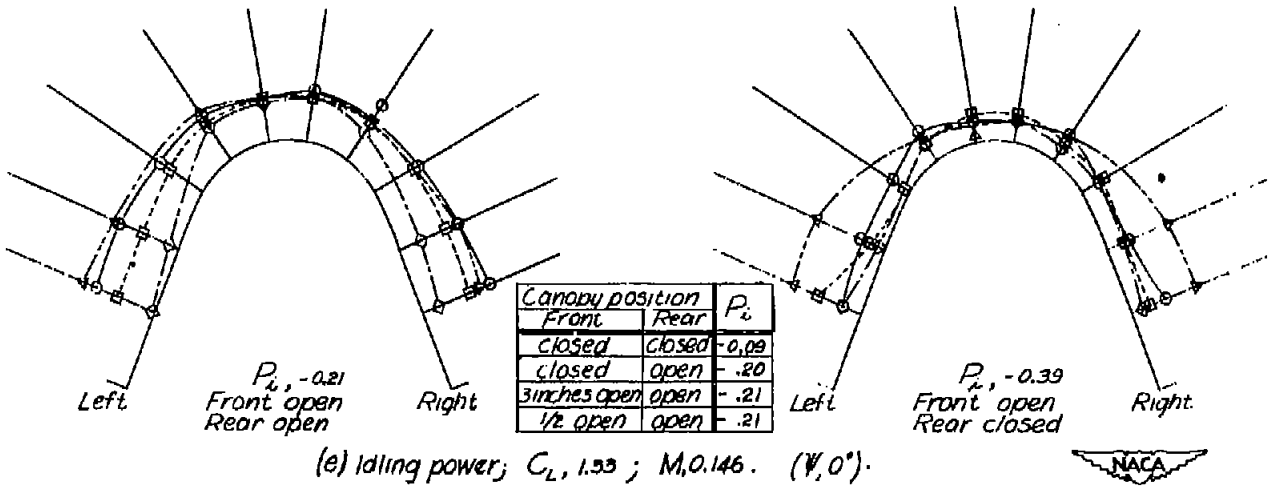

(e) Idling power; C_L, 1.53 ; M, 0.146 . (Ψ, 0°).

Figure 11.- Concluded.

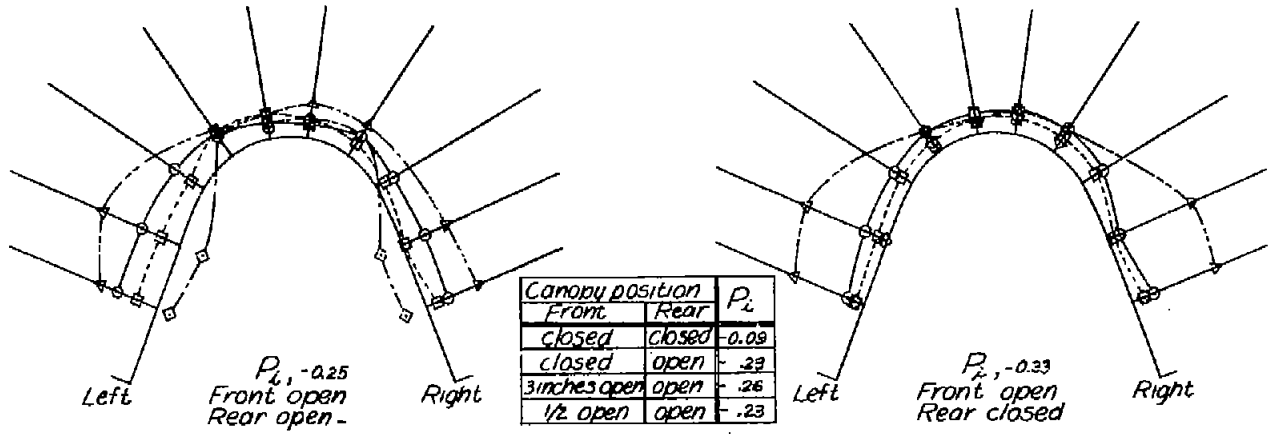

Canopy position		P_L
Front	Rear	
closed	closed	-0.09
closed	open	-.23
3 inches open	open	-.26
1/2 open	open	-.23

(a) Military power; C_L, 0.56; T_c, 0.16; M, 0.224.

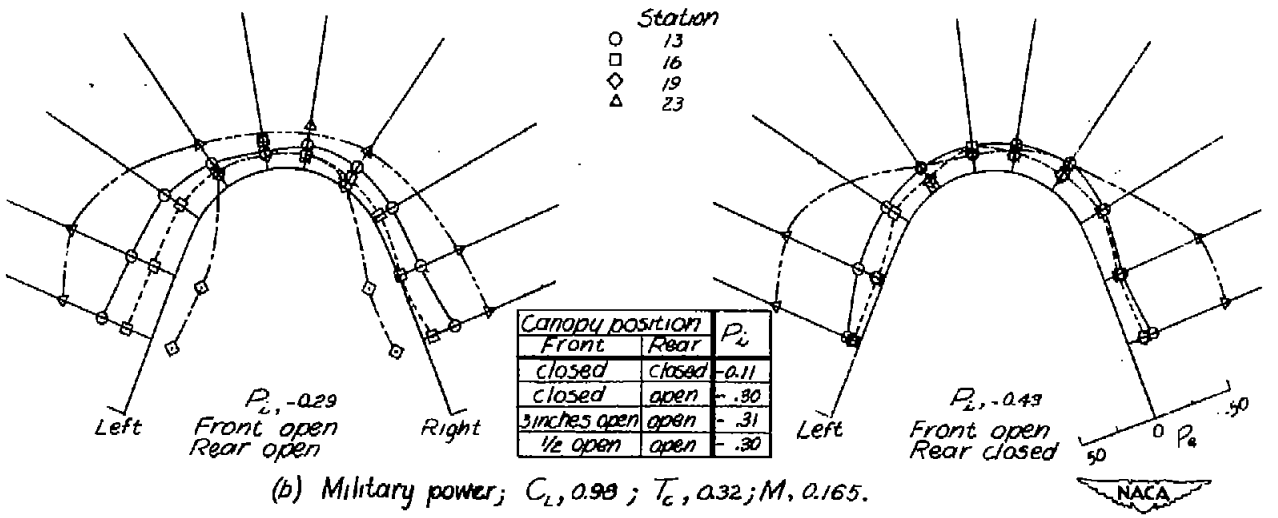

Canopy position		P_L
Front	Rear	
closed	closed	-0.11
closed	open	-.30
3 inches open	open	-.31
1/2 open	open	-.30

(b) Military power; C_L, 0.98; T_c, 0.32; M, 0.165.

Figure 12.- Pressure distributions over the rear canopy of the SB2C-4E airplane. $\Psi = -7.5^\circ$; h_p = 8000 feet.

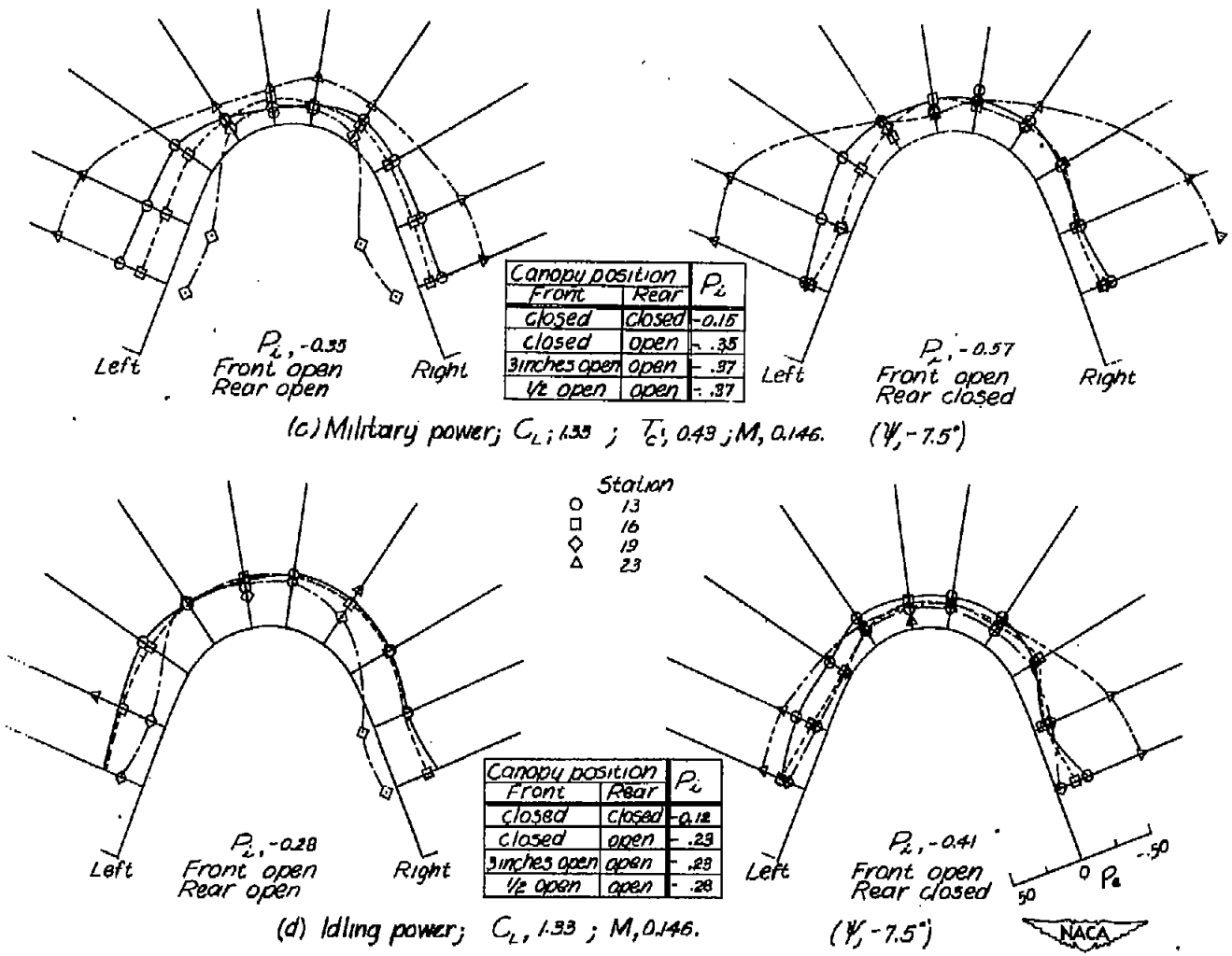

Figure 12.- Concluded.

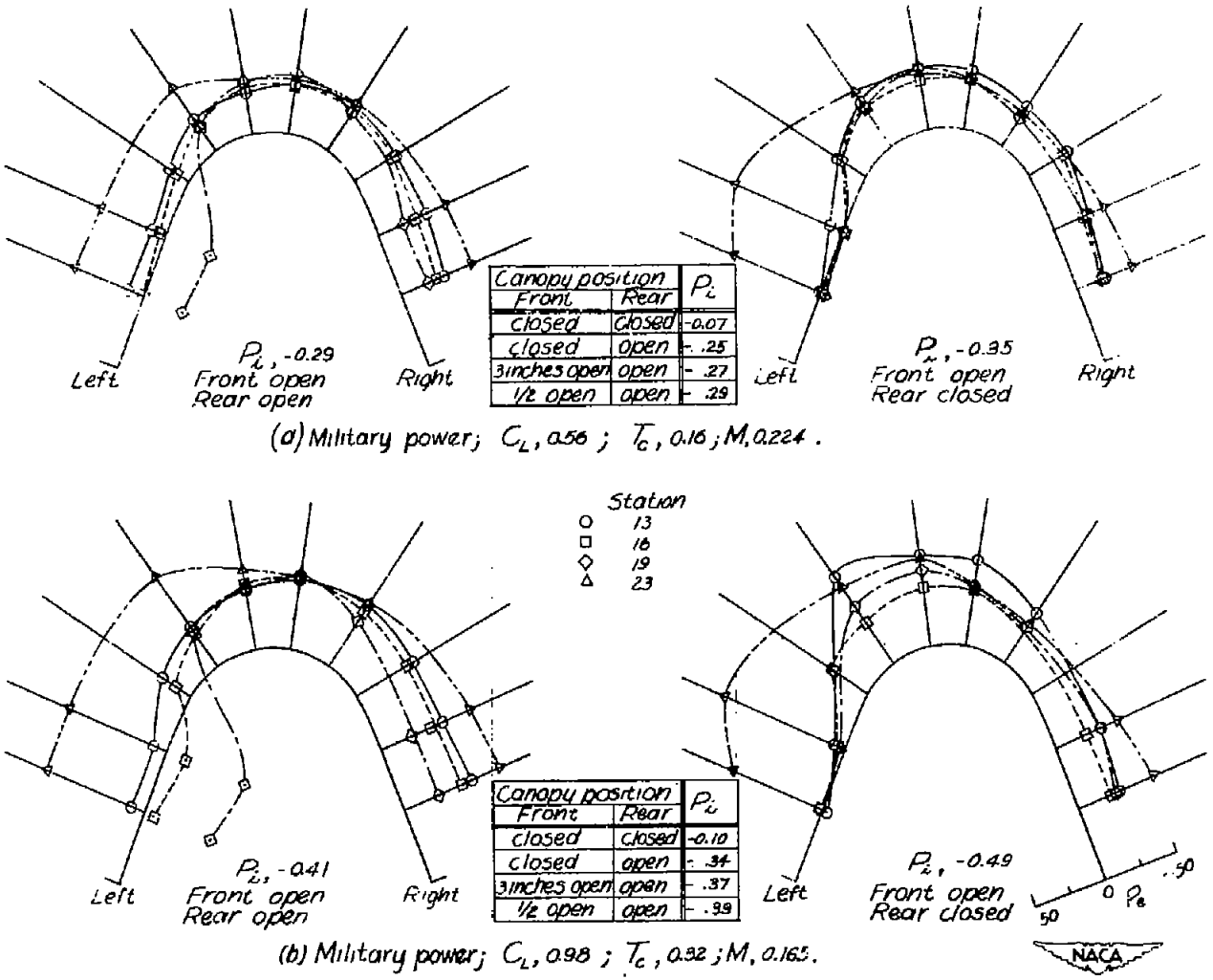

Figure 13.- Pressure distributions over the rear canopy of the SB2C-4E airplane. $\Psi = 7.5^{\circ}$; h_p = 8000 feet.

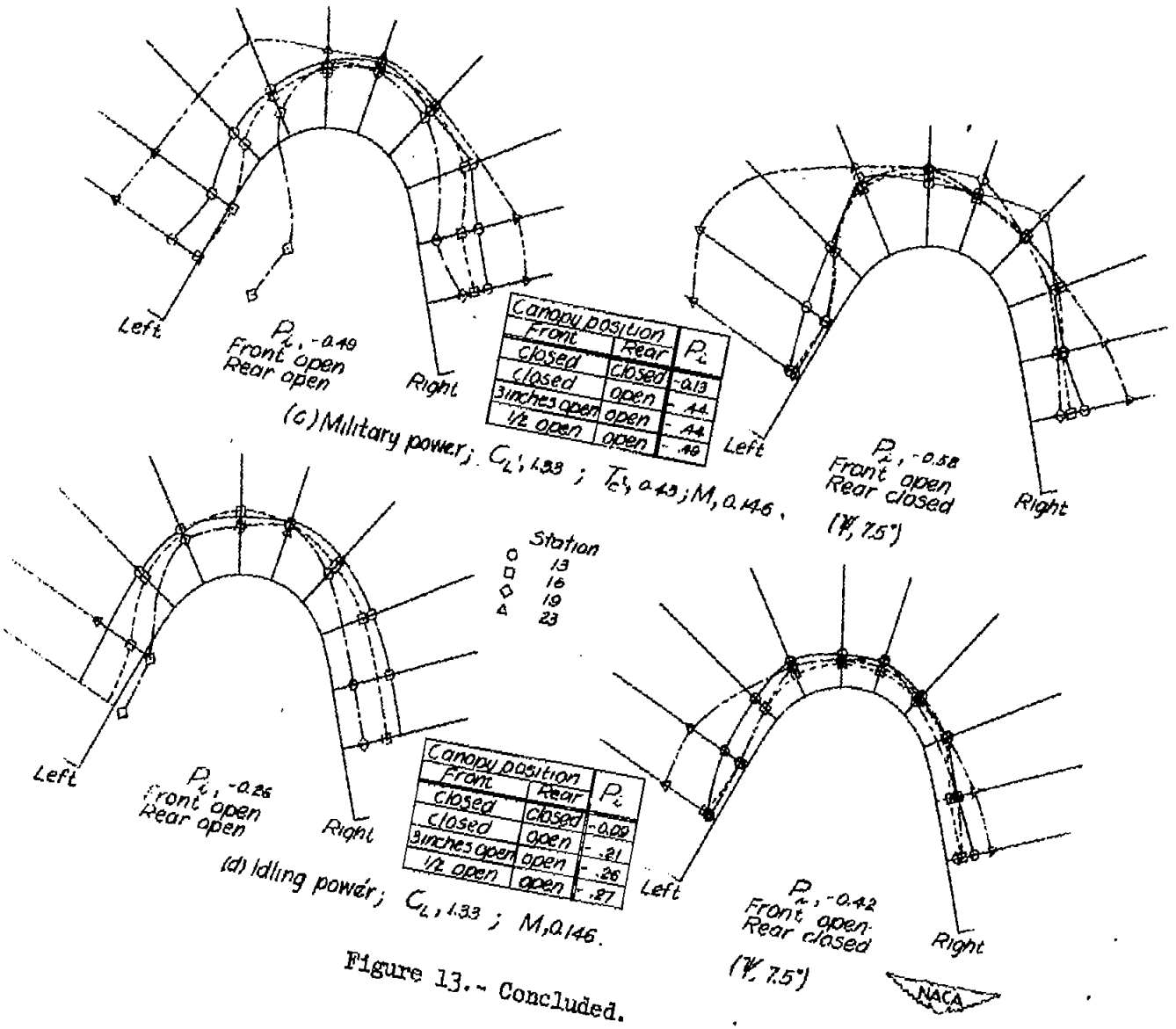

Figure 13.- Concluded.

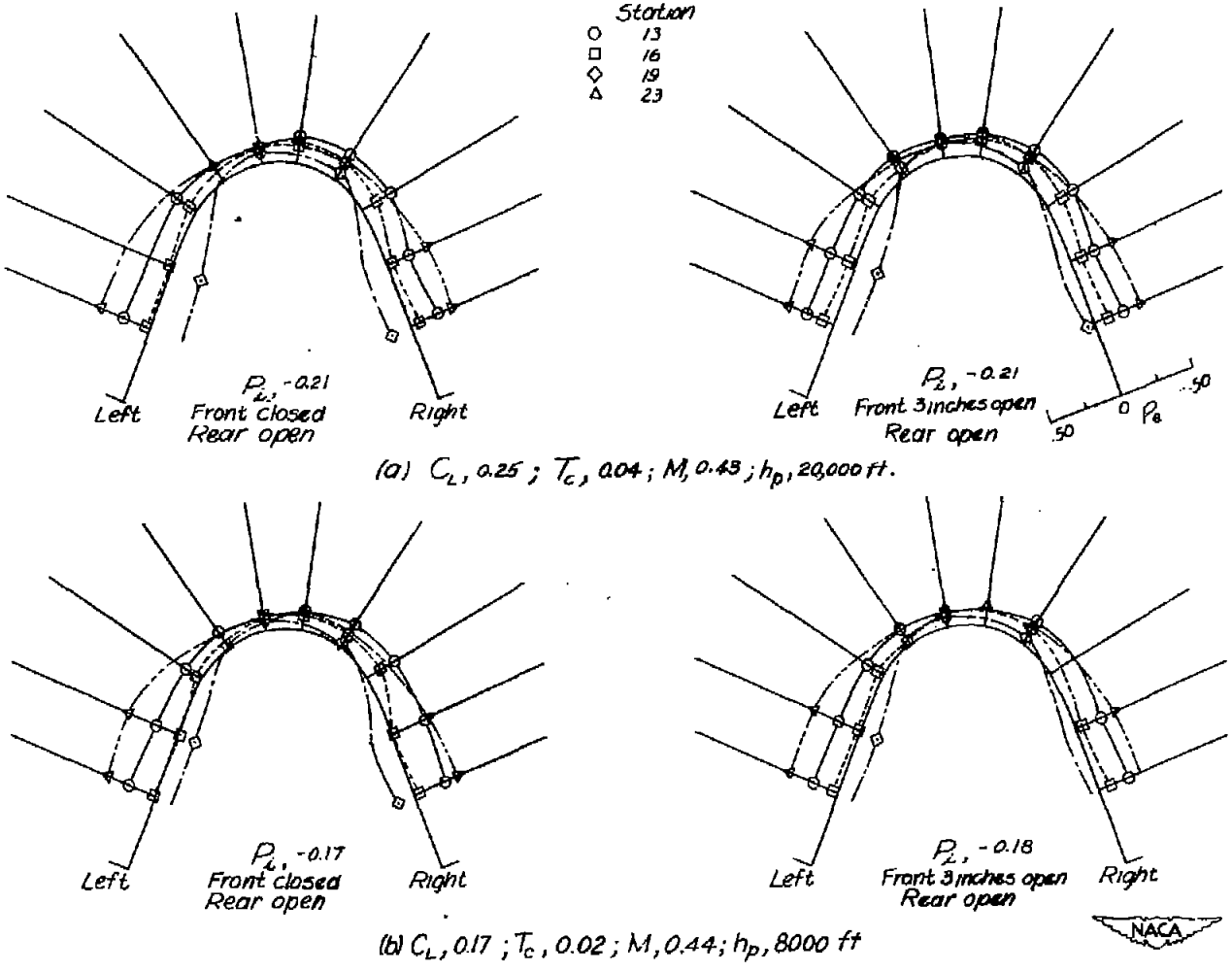

Figure 14.- Effect of distortion on the pressure distribution over the rear canopy of the SB2C-4E airplane. $\Psi = 0^\circ$; military power.

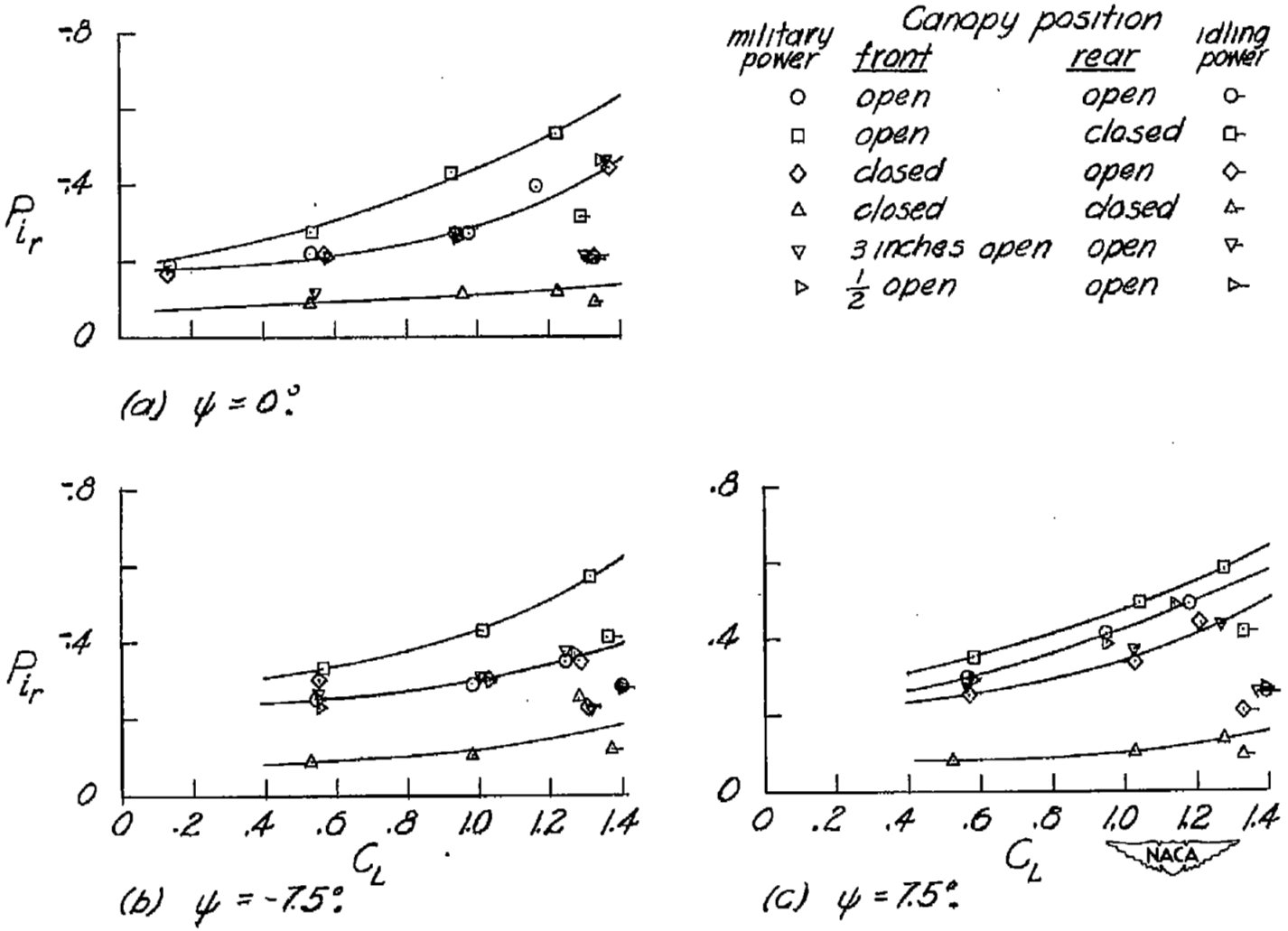

Figure 15.- Variation of rear canopy internal pressure coefficient with lift coefficient for various yaw angles, canopy positions, and power settings.

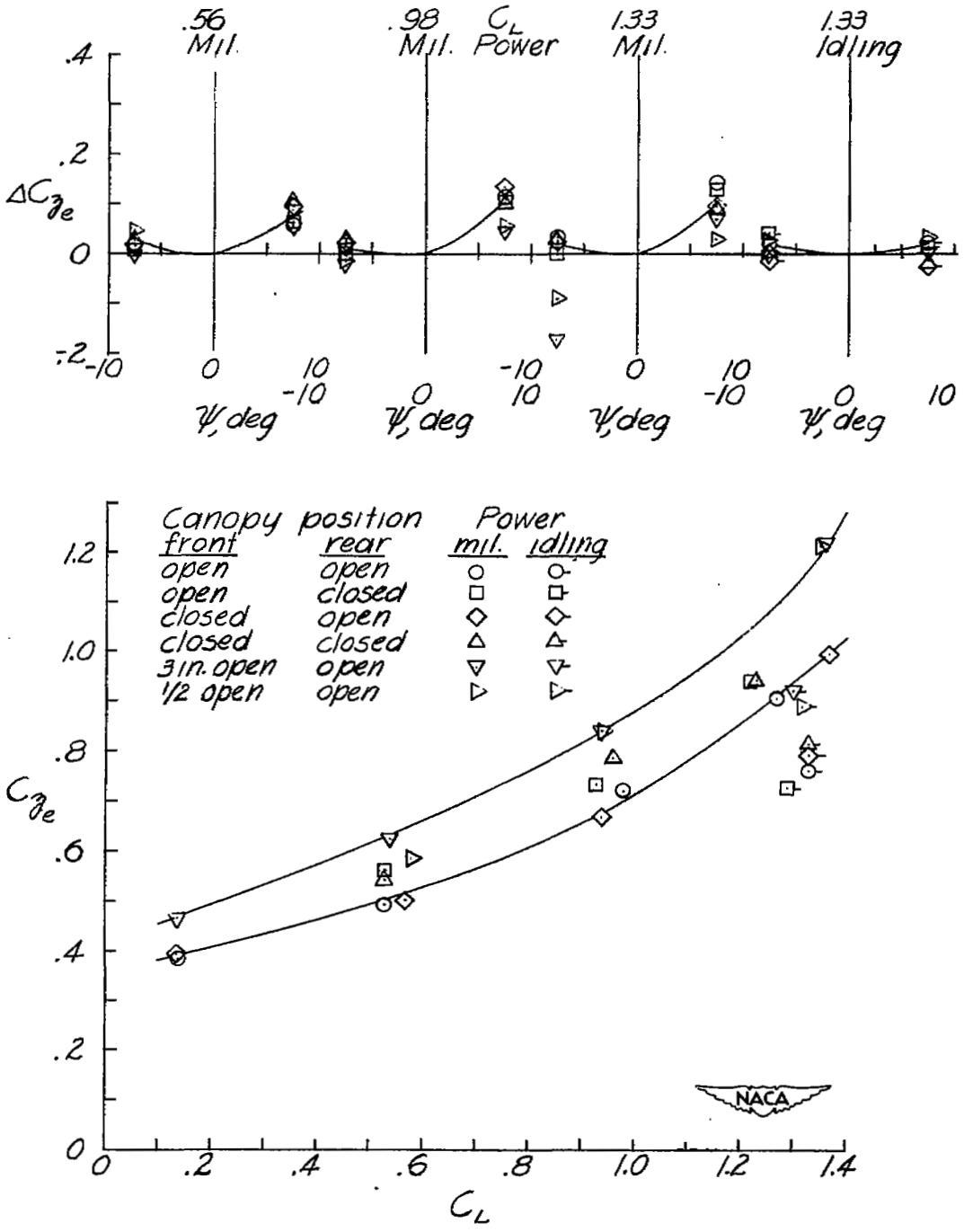

(a) External vertical load coefficient.

Figure 16.- Variation of front canopy load coefficient with lift coefficient and yaw angle for various canopy positions and power settings.

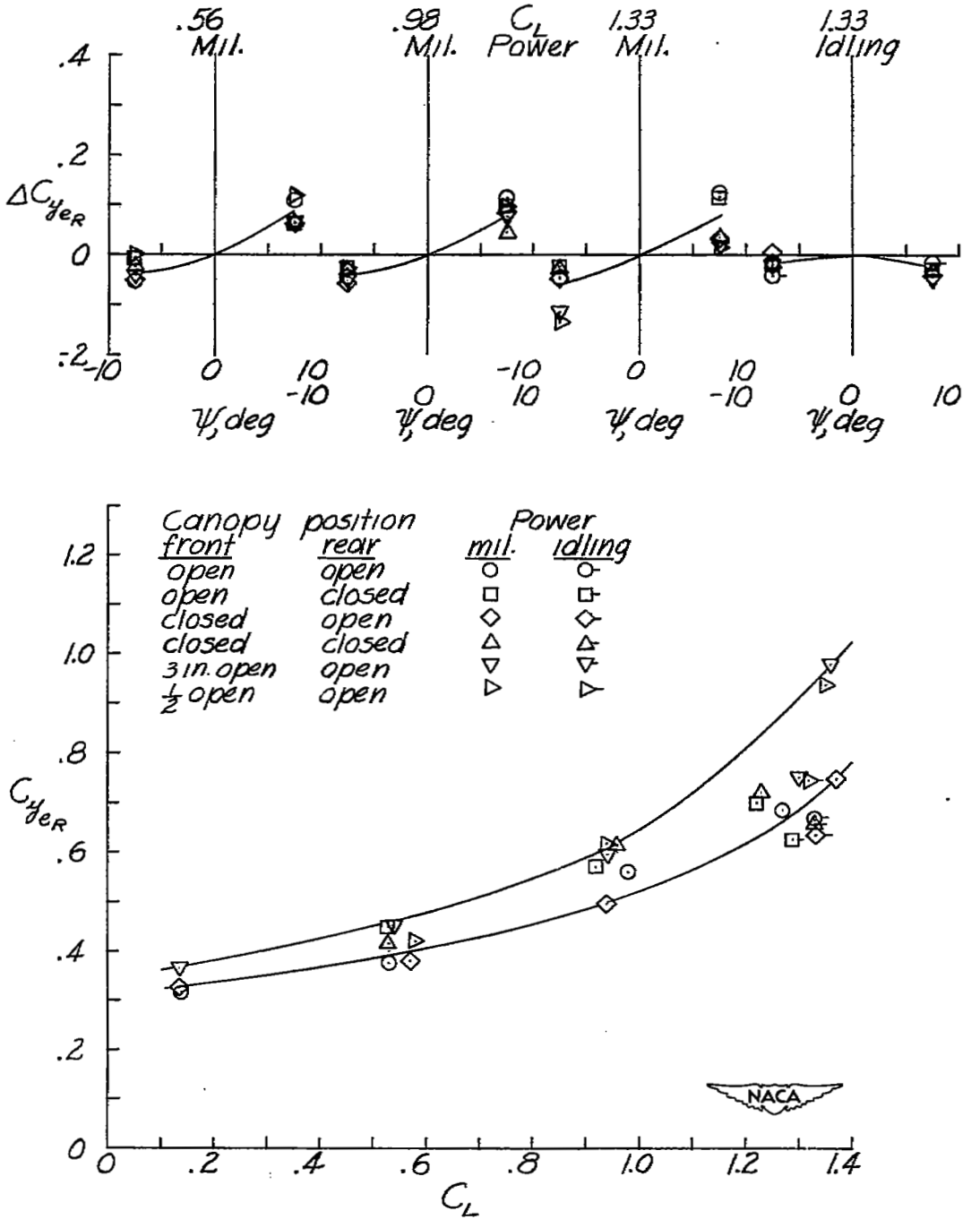

(b) External right lateral load coefficient.

Figure 16.- Continued.

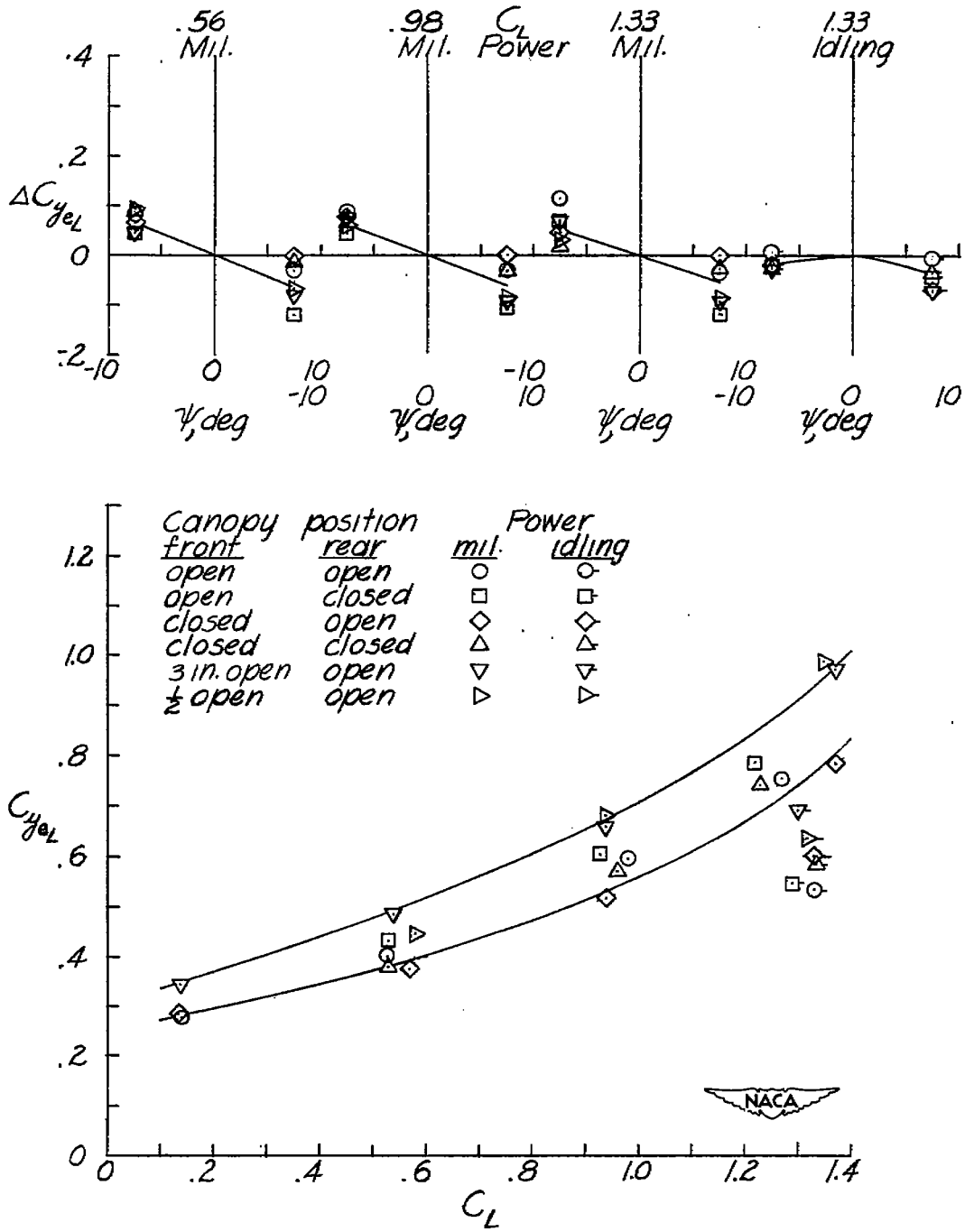

(c) External left lateral load coefficient.

Figure 16.- Continued.

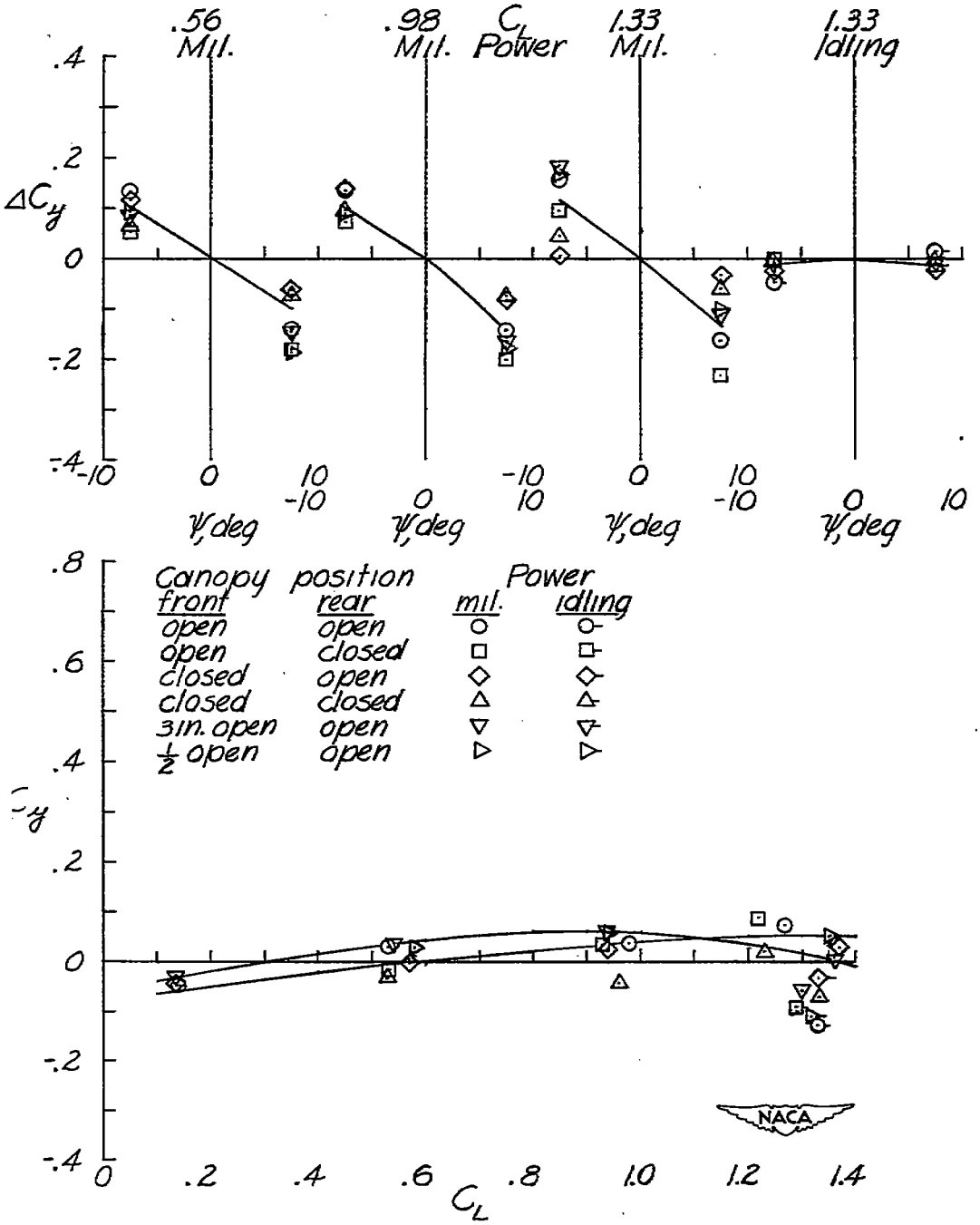

(d) Net external lateral load coefficient.

Figure 16.- Continued.

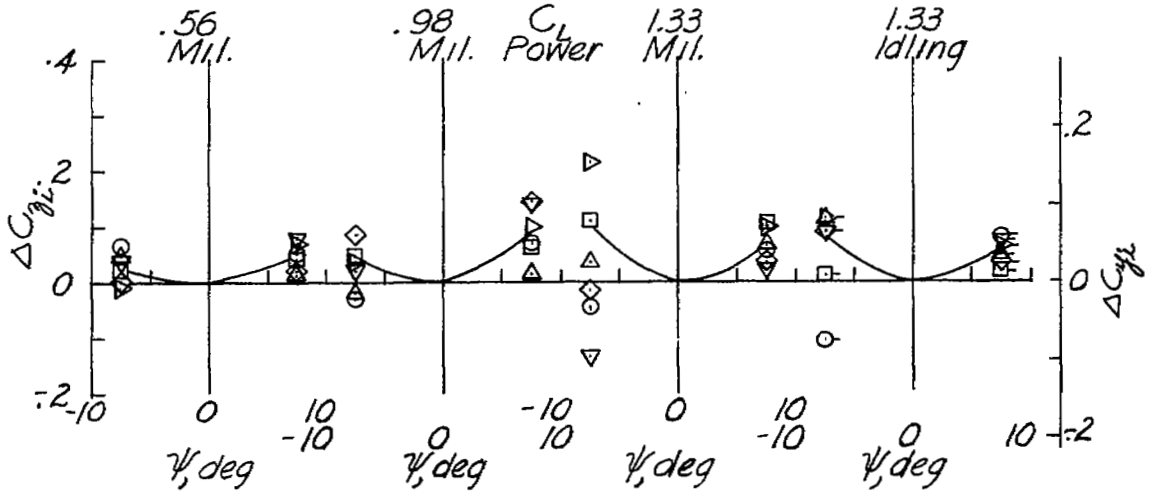

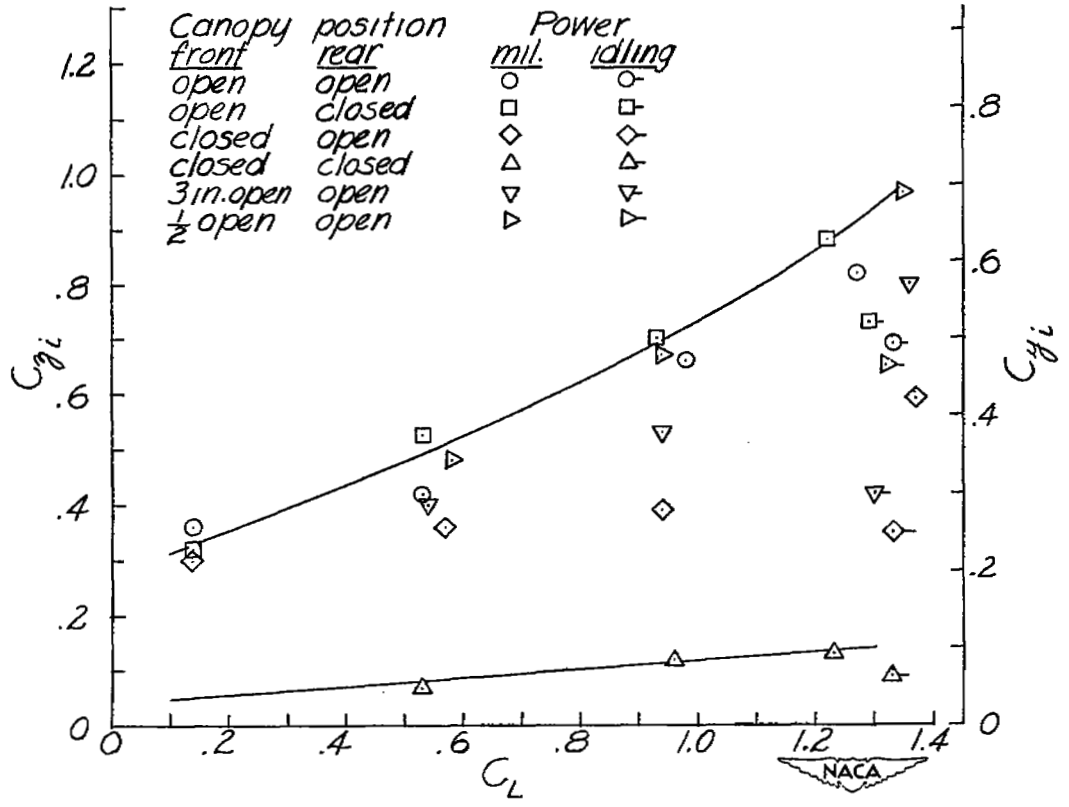

(e) Internal vertical and lateral load coefficient.

Figure 16.- Concluded.

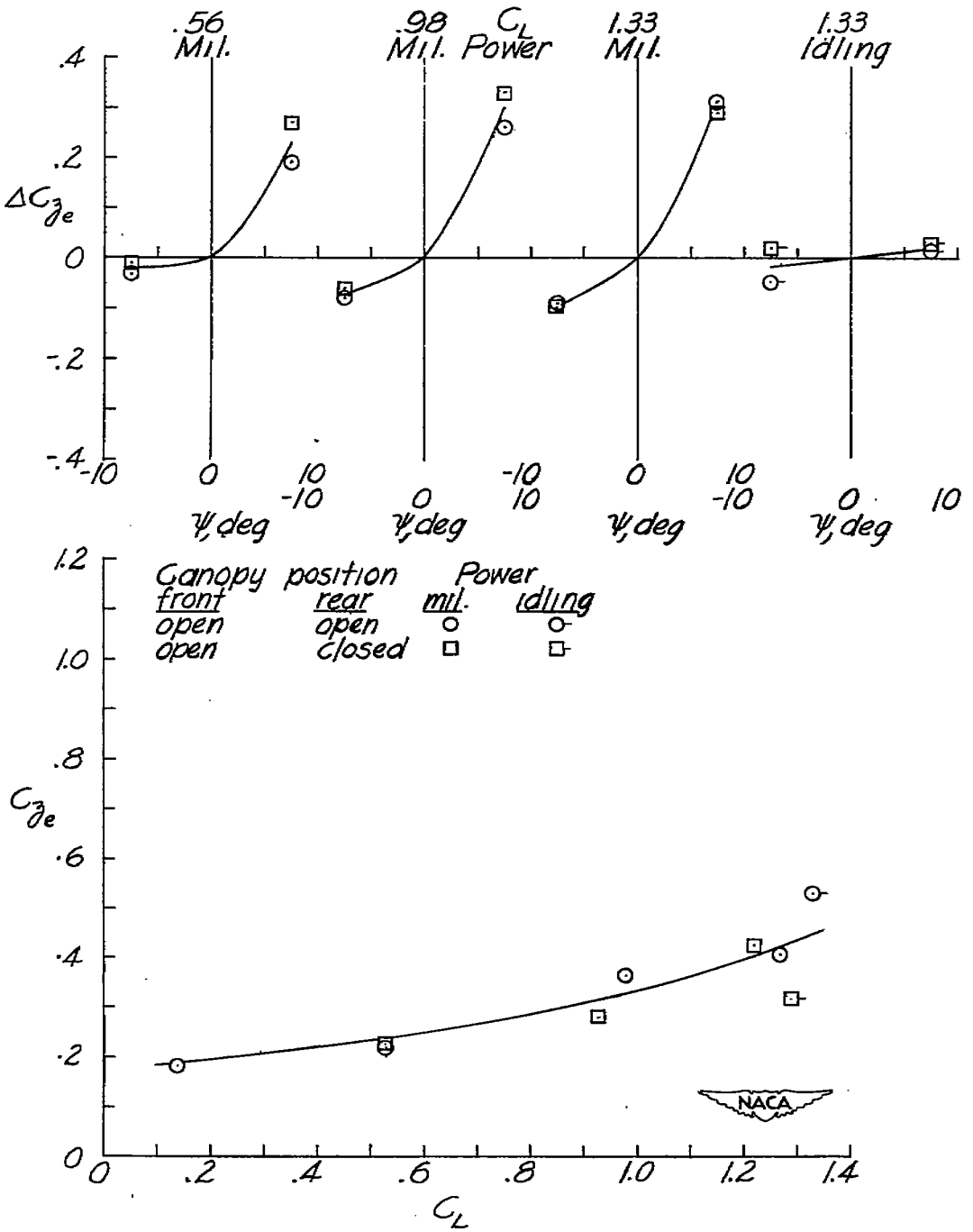

(a) External vertical load coefficient.

Figure 17.- Variation of rear-canopy load coefficient with lift coefficient and yaw angle for various canopy positions and power settings.

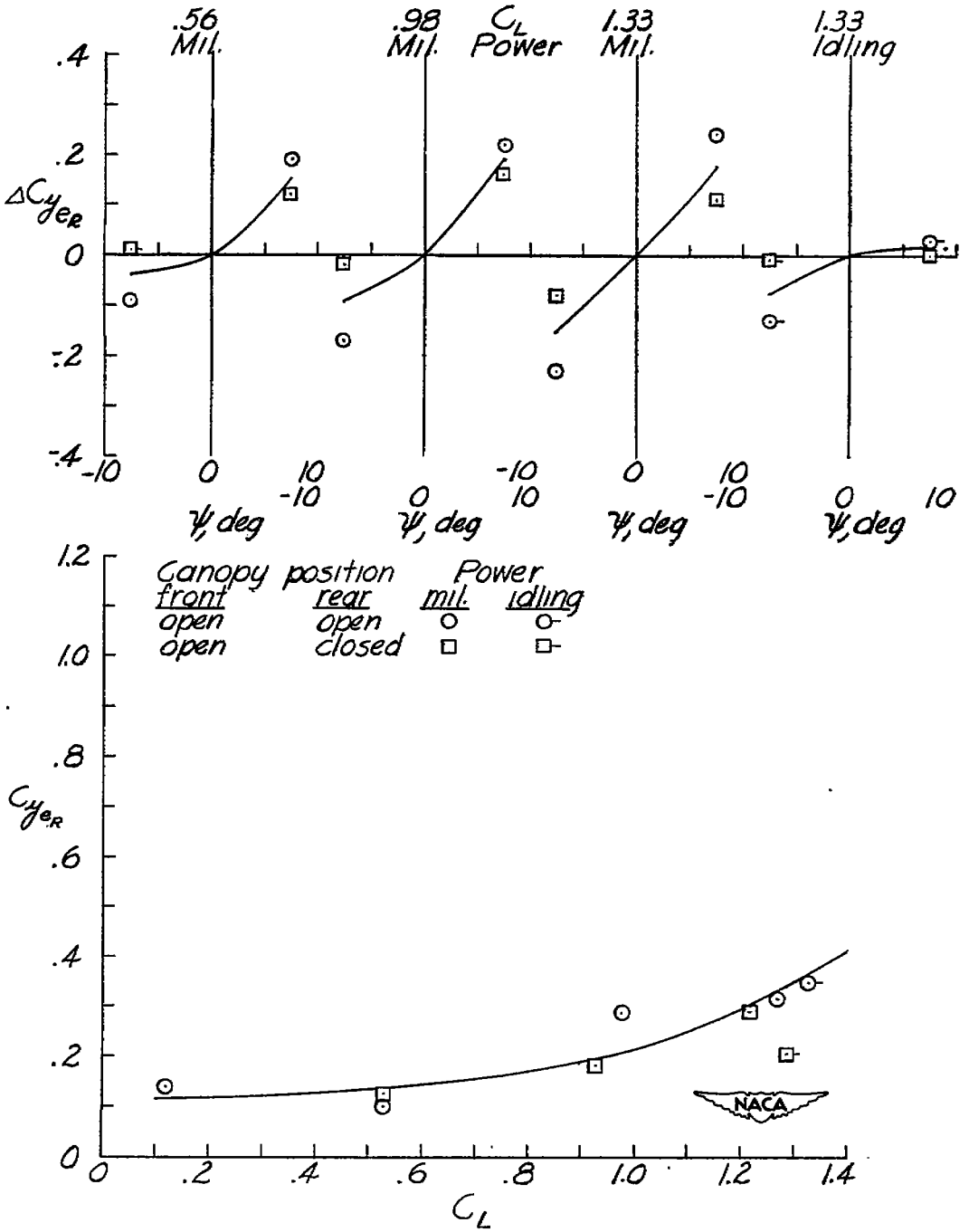

(b) External right lateral load coefficient.

Figure 17.- Continued.

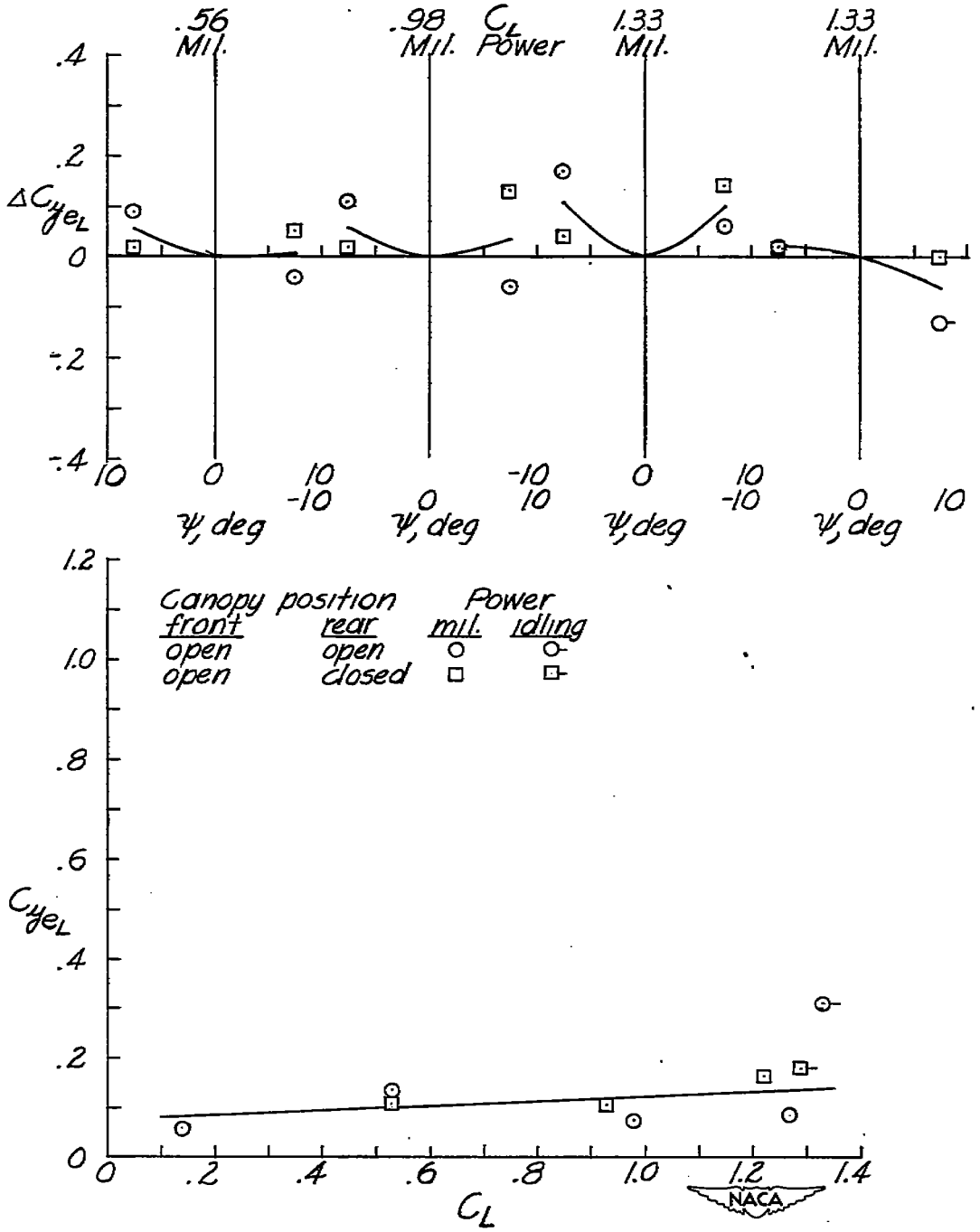

(c) External left lateral load coefficient.

Figure 17.- Continued.

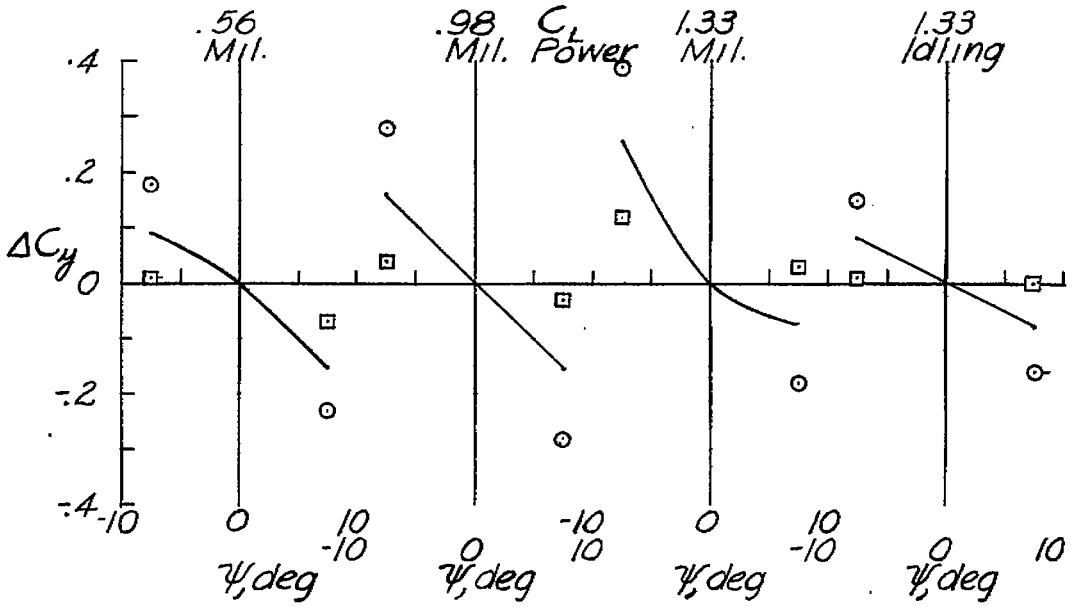

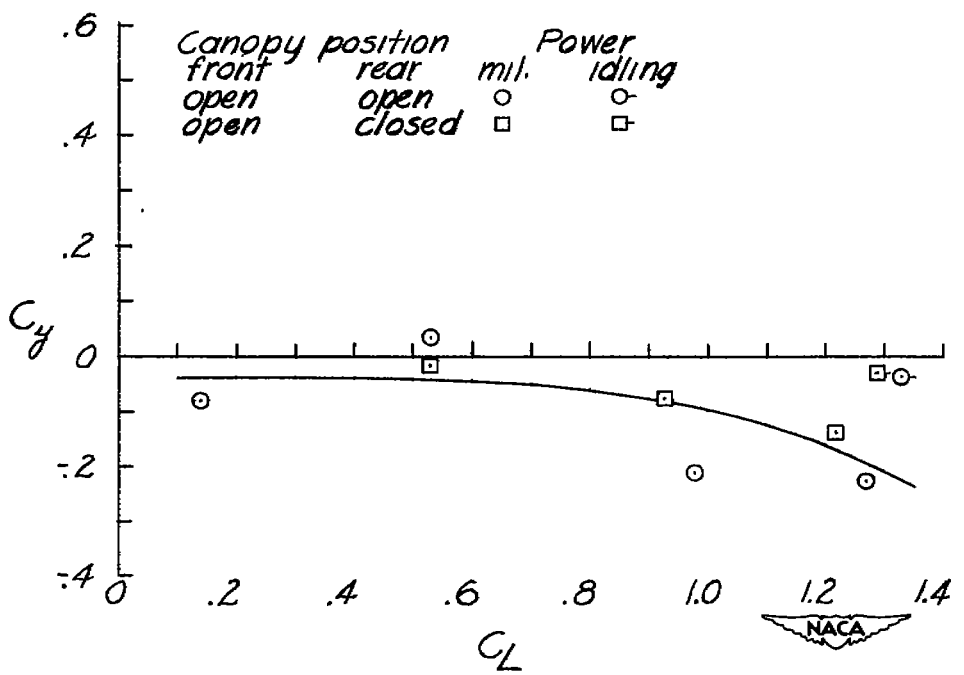

(d) Net external lateral load coefficient.

Figure 17.- Continued.

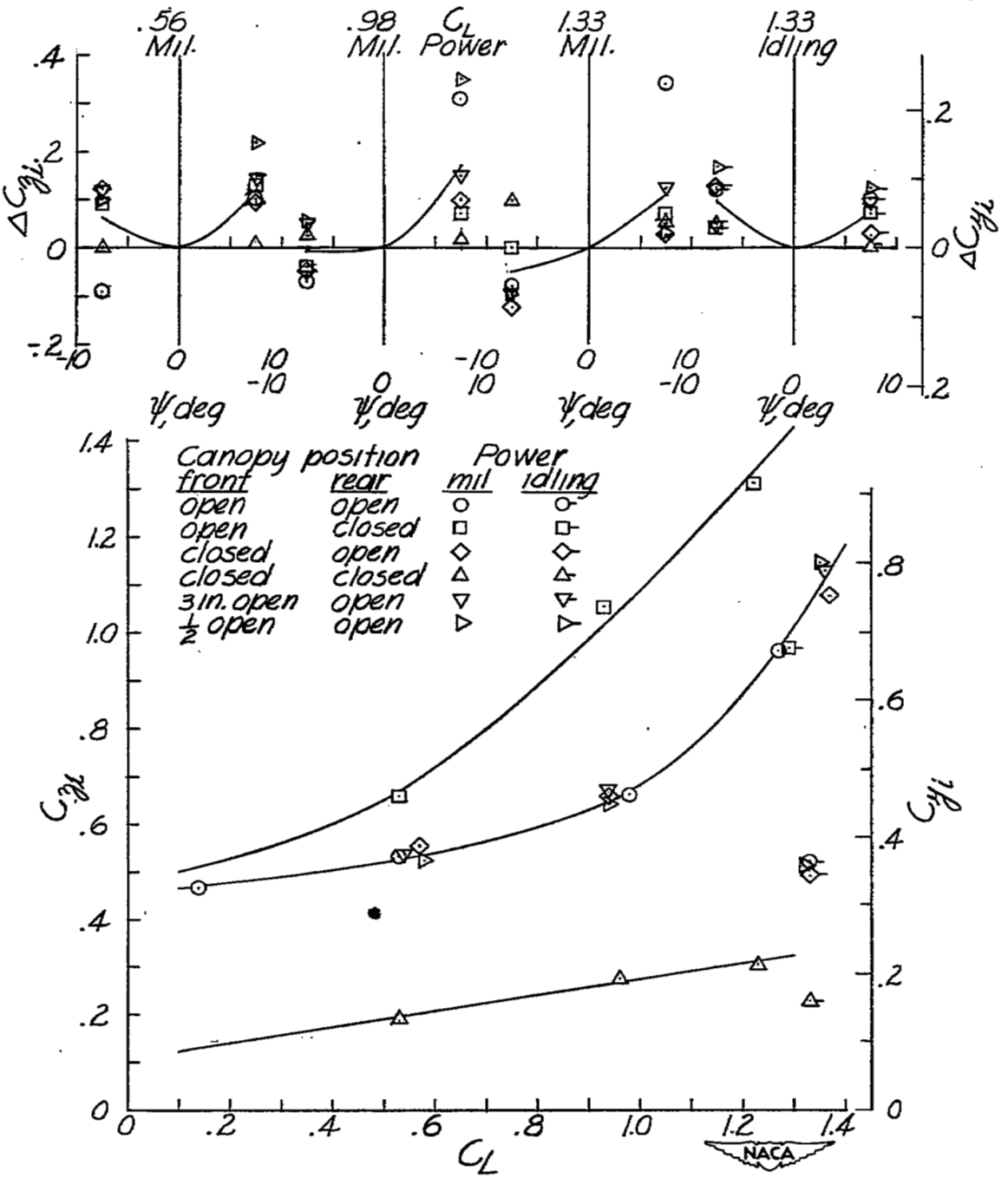

(e) Internal vertical and lateral load coefficient.

Figure 17.- Concluded.